ELSEVIER

Global and Planetary Change 30 (2001) 117–153

GLOBAL AND PLANETARY CHANGE

www.elsevier.com/locate/gloplacha

The two major warming phases of the last deglaciation at ∼14.7 and ∼11.5 ka cal BP in Europe: climate reconstructions and AGCM experiments

H. Renssen [a,b,*], R.F.B. Isarin [a]

[a] Netherlands Centre for Geo-ecological Research (ICG), Faculty of Earth Sciences, Vrije Universiteit Amsterdam, De Boelelaan 1085, NL-1081 HV Amsterdam, The Netherlands

[b] Institut d'Astronomie et de Géophysique Georges Lemaître, Université Catholique de Louvain, 2 Chemin du cyclotron, B-1348 Louvain-la-Neuve, Belgium

Received 16 June 2000; accepted 29 September 2000

Abstract

During the last deglaciation two distinct warming phases occurred in the N Atlantic region at ∼14.7 and ∼11.5 ka cal BP. These two shifts are the transitions from (1) GS-2a (Greenland Stadial 2a) to GI-1e (Greenland Interstadial 1e) and (2) GS-1 to the Preboreal. In this study we characterise these two important climate transitions by comparing maps of January and July temperatures for Europe acquired with two independent methods: (1) simulations with the ECHAM4 atmospheric general circulation model in T42 resolution and (2) temperature reconstructions based on geological and palaeoecological data. We also compare estimated lake level changes with simulated P-E (effective precipitation) values. These comparisons enable quantification of the climate change during the two phases. January temperatures increased by as much as 20°C in NW Europe from values between −25°C and −15°C in both GS-2a and GS-1 to temperatures between −5°C and 5°C in both GI-1e and the Preboreal. During July the changes were smaller, as the July temperatures increased in NW Europe by 3–5°C from about 10°C to 15°C in both GS-2a and GS-1 to values of 13°C to 17°C in both GI-1e and the Preboreal. In S Europe the increase in July temperature was less intense. Our analysis suggests that the effective precipitation remained at the same level during the 14.7 ka cal BP transition, whereas a small increase is inferred for some regions for the 11.5 ka cal BP shift. This small effect in effective precipitation is explained by comparable increases in precipitation and evaporation during both transitions. We infer that the strong increase in January temperatures was forced by changes in the N Atlantic Ocean, as the variations in sea surface temperatures and the position of the sea ice margin determined the temperature change over land. The increase in July temperatures was mainly driven by two factors: the increase in insolation and the deglaciation in Scotland and Scandinavia. The insolation changes were gradual (2 to 3 W/m^2) compared to the changes in the N Atlantic Ocean, explaining the relatively small temperature increase during July compared to January. In regions that were deglaciated during the two climate transitions, July temperatures appeared to have increased by up to 10°C. Our results suggest that the registration of the magnitude of the two climate shifts in terrestrial proxy records was geographically different due to the changing environmental conditions; variations in the N Atlantic sea ice limit appear to be the most

* Corresponding author. Netherlands Centre for Geo-ecological Research (ICG), Faculty of Earth Sciences, Vrije Universiteit Amsterdam, De Boelelaan 1085, 1081 HV, Amsterdam, The Netherlands. Tel.: +31-20-444-7357; fax: +31-20-646-2457.

E-mail address: Renh@geo.vu.nl (H. Renssen).

PII: S0921-8181(01)00082-0

important. This implies that reconstructed temperature curves from different places in Europe should show different magnitudes. Moreover, it is to be expected that the timing of the major warming phases is spatially different, as this timing is mainly determined by the position of the sea ice and land ice margins relative to the place of interest.

Keywords: climate change; general circulation model; simulation; reconstruction; Europe; Late-glacial; paleoclimate maps

1. Introduction

1.1. General outline

The last deglaciation is characterized by alternation of cold and warm climate intervals with very rapid transitions (e.g. Taylor et al., 1993a; von Grafenstein et al., 1999). The most distinct events are two major cold-to-warm transitions that occurred in the North Atlantic region at ~14.7 and ~11.5 ka cal BP (hereafter 'k'). These two phases are the transition from (1) the last part of the Weichselian Late Pleniglacial (sometimes referred to as the Oldest Dryas) to the Late-glacial Interstadial (often referred to as the Bølling–Allerød interstadial), and (2) the Younger Dryas stadial to the Preboreal. Both shifts are clearly registered in proxy records from the Greenland ice-sheets, such as oxygen isotopes and dust, and in European oxygen isotope records (Taylor et al., 1993b; von Grafenstein et al., 1999). These data suggest a very rapid transition from glacial to interglacial climate conditions, possibly within a few decades (Alley et al., 1993; Severinghaus and Brook, 1999). If we assume that the oxygen-isotope records are a proxy for Northern Hemisphere temperature, the isotope measurements suggest that the magnitude of the two warming phases may be comparable. However, during each of these transitions the Northern Hemispheric environmental situation was very different. During deglaciation (between these two transitions), the height of the ice sheets decreased significantly, insolation changed, the atmospheric CO_2 concentration increased and trees re-colonized the European continent (e.g. Berger, 1978; Barnola et al., 1987; Peltier, 1994; Hoek, 1997). Therefore, a comparison of these two transitional phases may provide valuable information on climate's sensitivity to rapidly changing boundary conditions. In this paper we study the climate of the 14.7 and 11.5 k warming phases in Europe using two independent methods: quantitative climate reconstructions based on multi-proxy records and simulations with an AGCM. Our aims are (1) to characterize quantitatively the climates in Europe during the two warming phases, and (2) to explore the impact of the various specific boundary conditions during these transitions.

1.2. Chronology and stratigraphy

One of the main problems when considering Late-glacial palaeodata is the definition and exact timing of the intervals before and after the 14.7 and 11.5 k isotopic shifts. Radiocarbon dating of these events is hindered by the presence of radiocarbon plateaux at 12.7, 10.4, 10.0 and 9.6 ^{14}C ka BP, thus centred around the main isotopic shifts (cf. Wohlfarth, 1996; Wastegård et al., 1998; Lowe et al., 1999). Furthermore, confusion arises when biostratigraphy, chronostratigraphy and lithostratigraphy are mixed (Lowe et al., 1995). In this paper, we therefore follow the event stratigraphy proposed by Björck et al. (1998) (see Fig. 1). Consequently, we use GS-2a for the last cold phase of the Pleniglacial, GI-1e for the first warm phase of the Late-glacial Interstadial (or 'Bølling') and GS-1 for the Younger Dryas stadial. In addition, we use PB to refer to the Preboreal.

1.3. Model studies

Various phases of the Late-glacial climate have been simulated in modeling studies. Simulations on the Younger Dryas climate have been performed by several groups (e.g. Rind et al., 1986; Renssen, 1997; Fawcett et al., 1997; Manabe and Stouffer, 1997; Mikolajewicz et al., 1997). The COHMAP group has been focusing on the warm phases before and after GS-1, i.e. at 14 and 11 k, and on the last cold phase at 16 k, before major warming started

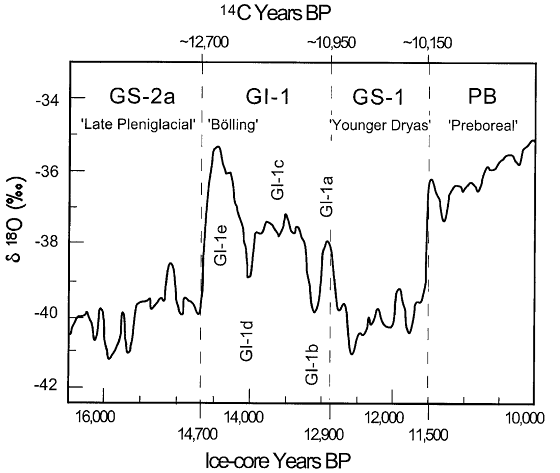

Fig. 1. Chronology of the Late Glacial following Björck et al. (1998). The solid line shows the $\delta^{18}O$ curve as measured in the GRIP Greenland ice core. GS-2a = Greenland Stadial 2a (Late Pleniglacial), GI-1e = Greenland Interstadial 1e ('Bølling'), GS-1 = Greenland Stadial 1 (Younger Dryas), PB = Preboreal.

(Kutzbach and Guetter, 1986; COHMAP, 1988; Wright et al., 1993; Kutzbach et al., 1998). These modeling studies provide important information on the factors that were driving climate around that time. For instance, simulations show that cooling in the N Atlantic Ocean and the associated sea ice extension played a dominant role during GS-1 and was the factor that forced the extremely low temperatures in Europe (Renssen et al., 1996; Isarin et al., 1998). In addition, model results indicate that the changing topography of the ice sheets in N America and Europe (i.e. lowering) caused a decrease in the intensity of the Jet stream over the N Atlantic (e.g. Webb et al., 1993; Felzer et al., 1998; Kageyama and Valdes, 2000). Also, the change in orbital forcing enabled the July temperatures in the early Late Glacial to reach values not too far from modern ones (Kutzbach et al., 1993). Although these modeling studies have provided new insights into the Late-glacial climate, they have not yet been used to study the character of the climate transitions.

1.4. Reconstructions

During the last decades, numerous palaeoecological and geological records containing information on the deglacial climate have been published. Based on the principle of modern analogues, these proxy records have been used to quantitatively reconstruct climate parameters for specific Late-glacial intervals. Emphasis has been on the reconstruction of temperatures. A number of large, continental-scale reconstructions based on mono-proxy records (e.g. Isarin, 1997; Isarin et al., 1997; Coope et al., 1998; Isarin and Bohncke, 1999) and multi-proxy records (Huijzer and Isarin, 1997; Huijzer and Vandenberghe, 1998) have become available. When stored in databases (e.g. European Pollen Database, Multi-Proxy DataBase, Lake Status Data Base) these data sets may serve as a tool for the construction of palaeoclimate maps. Unfortunately, reconstructions have till now focused primarily on NW Europe except for the Lake Status Data Base, which has Eurasian coverage (Yu and Harrison, 1995; Tarasov et al., 1996). Subsequently, palaeoclimate maps may be compared with the results of climate model experiments.

1.5. Data–model comparisons

Only a few model–data comparison studies have focused on the last deglaciation. Such a comparison of climate reconstructions with model results serves two major goals. First, it provides a necessary test for the model, and second, it improves our knowledge of the considered climate as it places the palaeodata in a physical context (Isarin and Renssen, 1999; Kohfeld and Harrison, 2000). COHMAP members (1988) used these principles to study the climates of the time-slices 21, 16, 14, 11 and 6 k, thereby revealing the effect of changes in ice sheets, insolation and other driving forces on climate since the last glacial (see also Wright et al., 1993). The study of COHMAP was recently updated by Kutzbach et al. (1998), who applied a more sophisticated model to simulate the climates of these time-slices. Moreover, they calculated the global distribution of biomes, which may be compared with palaeodata giving information on past vegetation. In earlier studies, we applied a model–data comparison to analyze the GS-1 (i.e. Younger Dryas) climate in Europe (Isarin et al., 1997; Renssen and Isarin 1998). This comparison provided valuable new insights. For instance, it revealed that the model produced anomalously high July temperatures over the European continent compared to the reconstructions. In a recent study we showed that this model–data mismatch was probably caused by the simplistic soil-module in the model, that was not able to reproduce permafrost in NW Europe (Renssen et al., 2000). In the present, paper we extend on our earlier work on the GS-1 climate by presenting simulated and reconstructed maps of climate for three additional time slices: GS-2a, GI-1e and PB.

2. Methods

2.1. Model experiments

2.1.1. Model

We applied the ECHAM-4 (European Centre/HAMburg) atmospheric general circulation model to perform our experiments. This model with 19 layers in the vertical is designed to simulate the atmospheric circulation at a sub-continental to a global scale. It calculates numerous climate parameters, including surface temperature, precipitation and wind strength and direction. The so-called T42 version of the model was used, which translates to a spatial resolution of $\sim 2.8 \times 2.8°$ of latitude–longitude. The main characteristics of present-day climate are satisfactorily reproduced by the ECHAM-4 model (Roeckner et al., 1996), which is an improved version of the model (ECHAM-3) we applied in earlier studies (Renssen et al., 1996; Isarin et al., 1997, 1998; Renssen, 1997; Renssen and Isarin, 1998). Nevertheless, several errors have been recognised. A known model bias for Europe includes the tendency to simulate anomalously high summer temperatures (+1°C difference with observations) and to underestimate summer precipitation (see Roeckner et al., 1996). A detailed description of the ECHAM model can be found in Roeckner et al. (1992, 1996) and DKRZ (1994).

Four palaeo-experiments were performed: two for cold phases (i.e. GS-2a and GS-1) and two for warm phases (i.e. GI-1e and PB). An overview of the experimental design is given in Table 1. Experiment CTRL is a control experiment, in which present-day boundary conditions are prescribed. The most important boundary conditions are ocean surface conditions (SSTs and sea ice), ice sheets, insolation, concentration of greenhouse gases and vegetation. In the other experiments these modern boundary conditions are adjusted to match the period of interest. As the simulations are designed as equilibrium experiments, we assume that these boundary conditions represent a characteristic mean state of the period of interest.

2.1.2. SSTs and sea ice

The ocean surface conditions of the palaeo-experiments are based on published reconstructions. For the Preboreal experiment (expPB), the modern set of sea surface temperatures (SSTs) was prescribed (see Fig. 2a and b) in accordance with the reconstructions of Schulz (1995), which show that the ocean surface conditions were very similar dur-

Table 1
Experimental design. The duration of the simulations is given in model years below the experiment names. The atmospheric concentration of CO_2 (ppm), CH_4 (ppb) and N_2O (ppb) is based on Antarctic ice core analyses by Raynaud et al. (1993)

	CTRL (15 years) Modern	expPB (12 years) 'Preboreal'	expGS-1[a] (12 years) 'Younger Dryas'	expGI-1e (12 years) 'Bølling'	expGS-2a (12 years) 'Late Pleniglacial'
SSTs + sea ice	0 k	0 k	GS-1 in N Atl. −2°C in N Pacific	GIN seas covered by sea ice	Global (CLIMAP[b])
Ice sheets	0 k	11 k	12 k	14 k	15 k
Insolation	0 k	11 k	12 k	14.5 k	15 k
$CO_2/CH_4/N_2O$	353/1720/310	260/720/270	246/500/265	220/650/220	220/450/220
Vegetation parameters	0 k	PB	'Younger Dryas'	'Bølling'	Glacial

[a] In expGS-1 a simple permafrost parameterization is included for regions with permafrost, consisting of two measures: (1) fixed frozen subsoil, (2) permanent high water table (see Renssen et al., 2000).

[b] For experiment expGS-2a we used the CLIMAP members (1981) SSTs except for the 'warm pools' in the Pacific that were removed. See text for further details on boundary conditions.

ing the early Preboreal (generally within 1°C, see Schulz, 1995). The SST set used in the YD simulation (expGS-1, see Fig. 2c and d) is identical to the one described in Renssen (1997). This data-set is based on model simulations of Schiller et al. (1997) and on SST reconstructions of Sarnthein et al. (1995). In the Bølling simulation (expGI-1e) we prescribed a cooling in the Greenland–Iceland–Norwegian (GIN) seas (see Fig. 2e and f), in accordance with SST reconstructions based on foraminifera (Schulz, 1995) and diatoms (Koç et al., 1993, 1996). South of Iceland ocean conditions were similar to those in CTRL. In the Late Pleniglacial simulation (expGS-2a) we used the set built by CLIMAP (1981) for the last glacial maximum (LGM, see Fig. 2g and h), but without the warm pools in the Pacific Ocean, since these are considered unrealistic (e.g. Rind and Peteet, 1985; Crowley, 1994; Guilderson et al., 1994). We are aware that the climate during our time-slice, i.e. 15 k, is not similar to that of the LGM (21 k). We have, however, two arguments that indicate that the CLIMAP-set is a reasonable approximation of the N Atlantic conditions just before the warming at 14.7 k. First, recent findings suggest that the CLIMAP-set is too cold for the LGM conditions in the GIN seas (Weinelt et al., 1996; de Vernal et al., 2000), and second, ocean core evidence shows that the N Atlantic was cooler between 16 and 14.7 k than during the LGM itself (e.g. Bond et al., 1993; Rasmussen et al., 1996a,b).

2.1.3. Ice sheets

The ice sheet extension and topography are shown in Fig. 2c–h and have been derived from Peltier (1994), who reconstructed ice sheet topography at thousand year intervals since 21 k. The elevations as provided on a 1° grid, were transformed to the T42-grid by linear interpolation, after which a smoothing function was applied to make the orography suitable for the ECHAM-4/T42 model. As seen in Fig. 2c–h, the extension of the Laurentide Ice sheet is not distinctly reduced going from 15 k to 12 k. However, the elevations drop from over 2000 to 1000 m, which indicates that considerable amounts of ice melted in four thousand years. The prescribed ice sheets for expPB are not shown here, since the ice sheet extensions are similar to that of expGS-1 (see Fig. 2c–d), whereas the elevation is lowered by a few hundred meters (see Peltier, 1994).

2.1.4. Insolation

During the Late Glacial the insolation in Europe was very different from today, with more incoming radiation in summer and less in winter. We prescribed the insolation on the basis of calculations made by Berger (1978). The deviation in insolation from present-day values (50°N: summer: 436 W/m^2, winter: 126 W/m^2) was at its maximum around the early PB (11 k). During summer the insolation anomaly was $+34$ W/m^2 at 50°N, whereas during winter it was about -11 W/m^2 at this same latitude. These differences compared to today are decreasing in value when going back in time (i.e. from 12 to 15 k). Compared to 0 k, the summer surplus values are as follows (50°N): 32 W/m^2 (12 k), 21 W/m^2 (14.5 k) and 18 W/m^2 (15 k). A similar trend, but with opposite sign, is evident for the winter radiation anomalies compared to 0 k: -10 W/m^2 (12 k), -6 W/m^2 (14.5 k) and -5 W/m^2 (15 k).

2.1.5. Vegetation parameters

In the ECHAM-4 model vegetation is important because it determines the characteristics of the earth surface through a number of parameters that are kept constant during a simulation. These parameters are surface background albedo, leaf area index (LAI), roughness length (Z_0), vegetation ratio and forest ratio (DKRZ, 1994). The vegetation ratio is the percentage of the ground covered with vegetation and consists of the average of the growing season and the season of dormancy. The forest ratio (i.e. percentage forest cover) is used to estimate the surface albedo of regions covered with trees, since the albedo of snow-covered forest is lower than that of snow-covered fields. In CTRL the data set of Claussen et al. (1994) is prescribed, who used the global modern vegetation as mapped by Olson et al. (1983) as a starting-point. For the palaeoexperiments we used the maps of Adams (1997), who reconstructed global vegetation for various time-slices from the LGM to the present based on published paleobotanical records. The procedure to translate the vegetation maps of Adams into data sets of land-surface

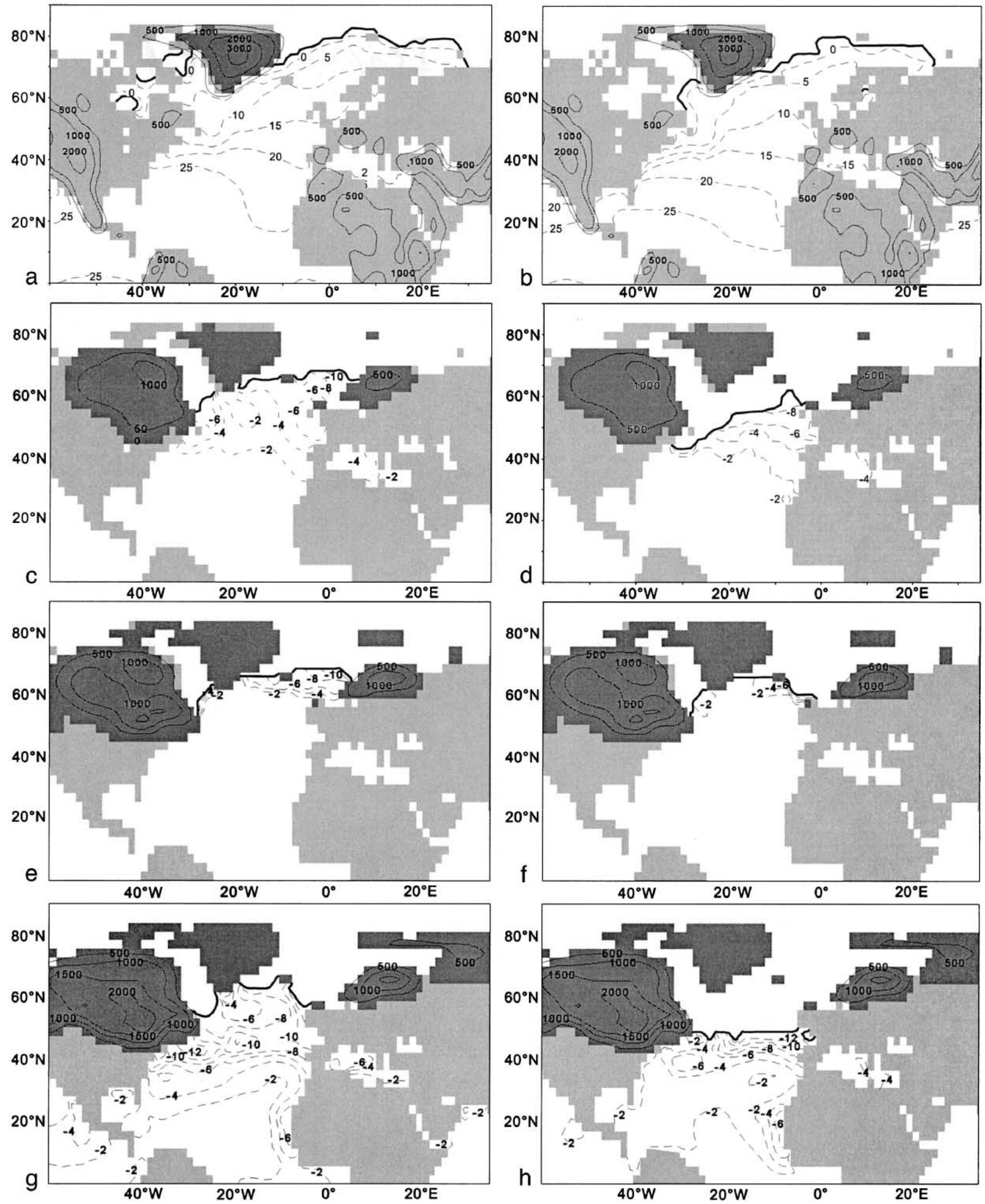
80°N
60°N
40°N
20°N
40°W
20°W
0°
20°E
a
b
c
d
e
f
g
h

parameters was as follows. First, we translated the vegetation types of Adams into the classes applied by Olson et al. (1983) and Claussen et al. (1994). Second, we coupled our classified vegetation maps to the data set of Claussen et al. (1994). This coupling enabled us to produce data sets for each palaeoexperiment for the five parameters (i.e. albedo, LAI, Z_0, vegetation ratio and forest ratio; see Renssen and Lautenschlager, 2000, for details).

2.2. Climate reconstructions

2.2.1. Methods of climate reconstruction

Various proxy records may be used to reconstruct climate quantitatively. The basic principle of reconstructing climate with proxy data is a comparison of the fossil distribution of, e.g. a periglacial phenomenon, a plant species or a specific beetle assemblage with their present-day distribution and related climate. So, the present is used to reconstruct the past. For example, the use of specific climate indicator plant species allows for an estimation of former mean temperatures of the coldest and warmest month (e.g. Iversen, 1954; Zagwijn, 1994; Isarin and Bohncke, 1999). The latter estimates are *minimum* (threshold) values indicating that true temperatures may have been higher. In addition, the mutual climatic range (MCR) of fossil insect assemblages enables quantitative estimates of both the warmest and coldest month (Atkinson et al., 1987; Coope et al., 1998). Beetle-based warmest month estimates are considered true values. Comparison between insect-based and plant-based temperature inferences for the Younger Dryas has suggested that the latter approximate true mean values (Isarin and Bohncke, 1999). Fossil periglacial features, such as ice-wedge casts and fossil frost mounds may be used to quantify past mean annual air temperatures and to give an indication of the mean coldest month temperatures (e.g. Vandenberghe and Pissart, 1993; Ballantyne and Harris, 1994; Isarin, 1997; Huijzer and Vandenberghe, 1998). Both reconstructed parameters are *maximum* values indicating that actual temperatures may have been below the inferred temperatures. Since biological and periglacial indicators to estimate January temperatures are limited, this parameter may be calculated using mean July and mean annual temperatures, and assuming a sinuous temperature curve (Isarin et al., 1998). We assume that, similar to today, July and January were the warmest and coldest months during the intervals under study. Whereas the reconstruction of former temperatures is relatively easy, estimation of former precipitation rates is more problematic. The status of lake levels may be regarded as the best proxy for the reconstruction of effective precipitation (e.g. Harrison and Digerfeldt, 1993). By looking at the change in lake level status between specific intervals, trends in lake status (stable, rising, falling) may be inferred.

We produced palaeoclimate maps for the selected intervals by using both available and newly compiled data sets of various origin. Combining multiple lines of evidence enables reconstruction of a large number of climate parameters (Huijzer and Isarin, 1997). In principle, the use of large data sets increases the reliability of the reconstructions. However, differences in quality of the data are present. Furthermore, it remains difficult to assess the errors associated with the estimates (see Isarin and Renssen (1999) for a discussion on data quality and errors). The majority of the reconstruction methods do not involve numerical statistics and consequently quantification of errors is difficult. Since estimates based on periglacial and botanical data are threshold values, uncertainty is introduced. Finally, it may be envisaged that some phenomena or species are better indicators for extreme events than for mean climate states.

Table 2 displays the data sets we used for the reconstruction. Occasionally, the existing data sets were updated with new information. Huijzer and Vandenberghe (1998) presented climate reconstructions for various time windows of the Weichselian.

Fig. 2. Land–sea–ice masks as prescribed in the model experiments (white = water, light grey = land, dark grey = land ice). Also shown are the sea surface temperatures (°C) and ice sheet elevations (m) as anomalies compared to the conditions prescribed for the modern climate ((a) July CTRL, (b) January CTRL). The thick line represents the southern sea ice margin. (c) July expGS-1, (d) January expGS-1, (e) July expGI-1e, (f) January expGI-1e, (g) July expGS-2a, (h) January expGS-2a. Contours for (a–b) at 5°C interval for SSTs and at levels 500, 1000, 2000 and 3000 m. Contour interval for (c–h) 2°C for SST anomalies and 500 m for elevation anomalies.

Table 2
Data sets used in this study. Ages of the intervals or status classes are in ^{14}C ka BP

	GS-2a	GI-1e	GS-1	PB
Huijzer and Vandenberghe (1998)	16.0–13.0			
Isarin (1997)			10.9–10.2	
Isarin and Bohncke (1999)			10.9–10.2	
Zagwijn (1994)				9.5
Yu and Harrison (1995) and Tarasov et al. (1996)	13.0	12.5	10.5	10.0
Coope et al. (1998)	14.5–13.0	13.0–12.5	11.0–10.0	10.0–9.0
Additional data	~ 14.0–12.7	~ 12.7–12.2	~ 10.9–10.2	~ 10.2–9.5

They tentatively subdivided their Late Pleniglacial periglacial data set in an early (20–16 ^{14}C ka BP) and later (16–13 ^{14}C ka BP) part. We used the latter data for the reconstruction of the maximum mean annual and January temperature during GS-2a. The pollen-based reconstruction of minimum mean July temperatures by Isarin and Bohncke (1999), as well as the January and annual temperature estimates from periglacial evidence of Isarin (1997), extended in Isarin et al. (1998), were used as a basis for the reconstruction of the thermal conditions during GS-1. We used the July and January estimates based on European pollen data by Zagwijn (1994) for the reconstruction of PB thermal conditions. Lake-level data from Yu and Harrison (1995) and Tarasov et al. (1996) were used as qualitative information on effective precipitation in the study area. In the latter databases, we looked at the changes in lake level status between the 13 and 12.5 ka BP (GS-2a to GI-1e transition) and between the 10.5 and 10.0 ka BP status classes (GS-1 to PB transition).

For regions not covered by the studies mentioned in Table 2 and for the GS-2a and GI-1e intervals, additional palaeobotanical information was collected primarily from literature (Fig. 3, Table 3). We used the method of climate indicator plant species to estimate temperature changes during the selected intervals (see Isarin and Bohncke, 1999, for a full description and discussion of the method). The botanical data set consists of 148 pollen diagrams from Europe. To assure regional coverage we included high-altitude sites, although we realise that differences in exposition in mountain areas may lead to ambiguous interpretations. In general, the analysis of climate indicator species was based on pollen and plant macrofossil diagrams presented in publications. In addition, we used data from the European Pollen Database (EPD, accessed via the National Geophysical Data Center, NOAA). The advantage of using the original counts is that indicator species not shown in the pollen diagrams can be included in the analysis. The biozonation proposed by the original author was checked and if necessary the stratigraphy was re-interpreted. We assume that GS-2a is equivalent to biozone Ia, GI-1e to biozone 1b, GS-1 to biozone III and the PB to biozone IV. In the diagrams, we looked for the presence of climate indicator plant species during these biozones. We concentrated on the spectra near the biozone boundaries. Appendix A shows the selected sites and references with indication of the local pollen zones as well as the use of EPD data.

To examine the consistency of our pollen-based temperature estimates, we compared our reconstructions with estimates of the mean temperature of the warmest month based on beetle evidence processed with the Mutual Climatic Range method (MCR, Atkinson et al., 1987). Recently, Coope et al. (1998) provided reconstructions based on data from 78 NW European sites. Estimates are given for 500 ^{14}C year intervals covering the 14,000 to 9000 ^{14}C BP interval. The MCR sites are mainly located in the British Isles and Sweden.

Before proceeding, some chronological aspects need consideration. Establishing time control of palaeoecological and geological records, which is essential for reconstructions, may be problematic. Due to geographical position, the expression of climate changes in pollen records differs throughout the study area. Especially for the intervals selected in

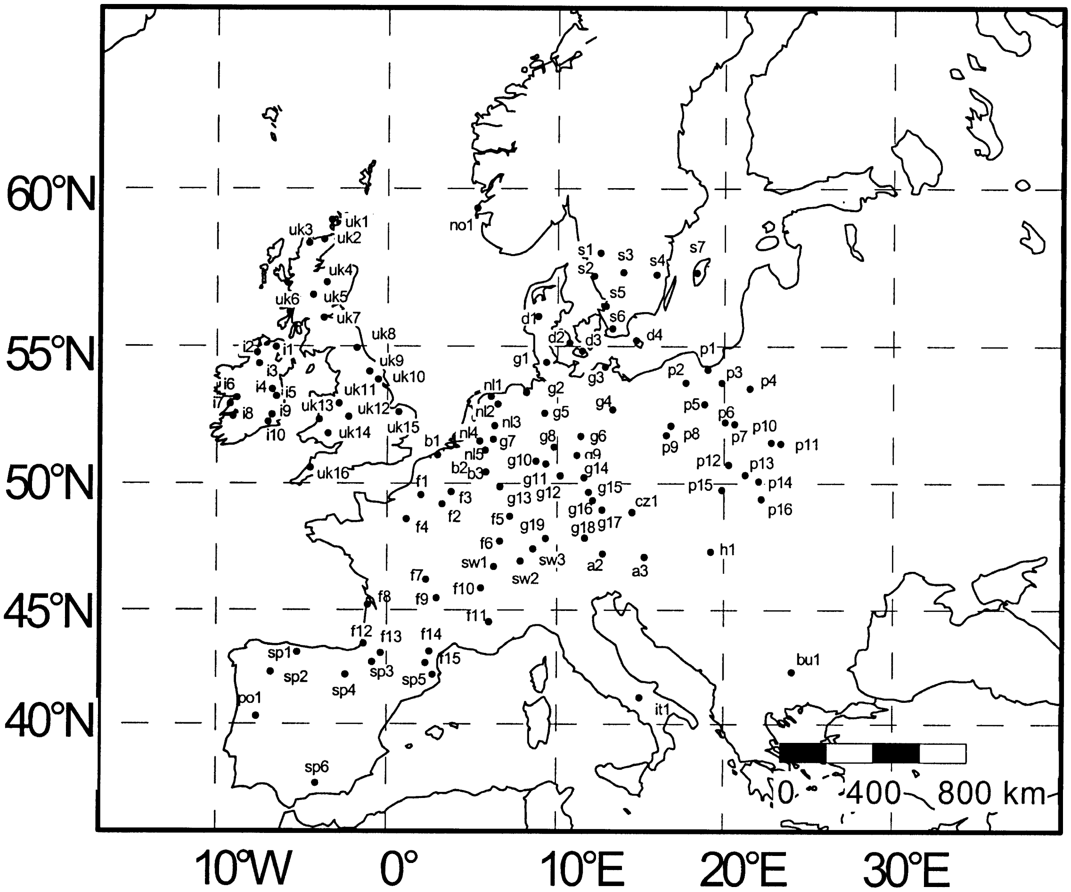

Fig. 3. Study area with palaeobotanical sites (additional data set). Codes correspond with Table 3.

this study, radiocarbon dating hinders establishing the chronology of events (cf. Wohlfarth, 1996). Clearly, the presence of radiocarbon plateaux is linked to periods of rapid climate change. Due to the scarcity of organic matter, time control of periglacial features from GS-2a relies on their stratigraphical position. An important and useful time-marker frequently observed in the NW European lowland is the Beuningen Gravel Bed. This stratigraphical horizon has recently been OSL dated to ~16 k (Bateman and Van Huissteden, 1999). However, in many cases this marker is absent, thus leaving periglacial features relatively poorly dated.

2.2.2. Model–data comparison

In this paper we compare simulated and reconstructed maps of July and January average temperatures for the four time-slices (i.e. GS-2a, GI-1e, GS-1 and PB), as well as the GI-1e–GS-2a and PB–GS-1 anomalies. The latter figures give an estimate of the temperature change during the 14.7 and 11.5 k transitions. In addition, simulated maps of the 'effective precipitation' (i.e. mean annual P-E) anomalies are shown that may be compared with reconstructed lake level trends for the two transitions. We have chosen July and January temperatures and effective precipitation, because these parameters can be estimated from proxy data. The simulated July mean values are compared with the reconstructed July estimates. Similarly, we compare the model result for January with the reconstructed January temperatures. The presented simulated temperatures are based on values initially calculated at 2 m above the earth surface and are taken as the seasonal

Table 3
Additional palaeobotanical sites. Codes refer to Fig. 3. Altitudes below 100 m a.s.l. not specified. For references see Appendix A

CODE		Refs.	
Norway			
n1*	SW Norway	Paus (1988, 1989)	
Sweden			
s1	Björkeröds mosse	Liedberg-Jönsson (1988)	EPD
s2	L. Sambösjön	Digerfeldt (1982)	EPD
s3	Akerhultagöl 303	Bjelm (1976) Björck and Håkansson (1982)	EPD
s4	Skvarran	Svensson (1989)	EPD
s5	Håkulls mosse	Berglund and Ralska Jasiewiczowa (1986)	
s6	Toppeladugård	Liedberg-Jönsson (1988)	
s7	Lösensjön	Berglund (1966)	
s8	Stangsmyr	Svensson (1989)	EPD
Denmark			
d1	Böllingsö	Stockmar (1974)	
d2	L. Flådet	Fredskild (1975)	
d3	Graenge	Kolstrup and Buchardt (1982)	
d4	Vallensgard Mose 100	Iversen (1954), Usinger (1977)	
United Kingdom			
uk1*	Orkney Islands	Moar (1969a,b)	EPD
uk2	L. of Winless	Peglar (1979)	
uk3	Cross Loch	Charman (1994)	
uk4	Morrone 425	Huntley (1994)	EPD
uk5	Tynaspirit 300	Lowe and Walker (1977)	
uk6	Drimnagall	Rymer (1977)	
uk7	Baenrig Moss 250	Webb and Moore (1982)	EPD
uk8*	NE England	Bartley et al. (1976), Jones (1976), Day (1995)	
uk9	Tadcaster	Bartley (1962)	EPD
uk10	Bog Roos	Beckett (1981)	EPD
uk11	Cross mere	Beales (1980)	
uk12	Kings Pool	Bartley and Morgan (1990)	EPD
uk13	Elan Valley	Moore (1970)	
uk14	Traeth Mawr 330/Llanilid	Walker (1982), Walker and Harkness (1990)	EPD
uk15	Hockham mere	Bennett (1983)	EPD
uk16	Hawks Tor	Brown (1977)	EPD
Ireland			
i1	Sluggan Bog	Smith and Goddard (1991)	
i2	Meenadoan	Pilcher and Larmour (1982)	
i3	Drumurcher	Coope et al. (1979)	EPD
i4	Dunshauglin	Mitchell (1940), Watts 1977	EPD
i5	Ballybetagh 250	Watts (1977), Cwynar and Watts (1989)	EPD
i6	Lurga	Andrieu et al. (1993)	
i7	Lough Goller 150	Watts (1963, 1977)	EPD
i8	Tory Hill	O'Connell et al. (1999)	
i9	Coolteen	Craig (1978)	EPD
i10	Belle lake	Craig (1978)	EPD
Netherlands			
nl1	Waskemeer	Casparie and Van Zeist (1960)	
nl2	Uteringsveen	Cleveringa et al. (1977)	
nl3	Usselo	Van Geel et al. (1989)	

Table 3 (*continued*)

CODE		Refs.	
Netherlands			
nl4	Milheeze	Bos (1998)	
nl5	Gulickshof/Putbroek	Hoek et al. (1999), Jansen and IJzermans-Lutgerhorst (1973)	
Belgium			
b1*	W. Belgium	Verbruggen (1979)	EPD
b2	Petite Nethe	Munaut and Paulissen (1973)	
b3	Konnerzvenn 580	Woillard (1975)	
France			
f1	Bresles	Van Zeist and Van der Spoel-Walvius (1980)	EPD
f2	Coizard Joches	Van Zeist and Van der Spoel-Walvius (1980)	EPD
f3	Chivres	Van Zeist and Van der Spoel-Walvius (1980)	EPD
f4	T. de l’Archet	Jalut (1967)	
f5	Frère Joseph 850	Woillard (1975)	
f6	Lac Sewen 501	Schloss (1979)	
f7	Lac Noir 840	Guenet (1993)	
f8	Lède de Gurp	Marambat and Roussot-Larrogue (1989)	
f9	Ampoix 1015	De Beaulieu and Goeury (1987)	EPD
f10*	Bas-Dauphinois	Wegmüller (1977), Clerc (1988)	EPD
f11*	Haute Provence	De Beaulieu (1977)	EPD
f12	Le Moura	Oldfield (1964), Reille (1993)	
f13	Estarrès (356)	Jalut et al. (1992)	
f14	Abeurador, Font Juvénal	Heinz and Thiébault (1998)	
f15*	E. Pyrenees	Reille and Lowe (1993), Jalut et al. (1982)	
Portugal			
po1	Charco da Candieira 1409	Van der Knaap and Van Leeuwen 1997	
Spain			
sp1	Lago de Ajo 1570	Allen et al. (1996)	EPD
sp2	Sanabria 1050	Hannon (1985), Allen et al. (1996), Turner and Hannon (1988)	EPD
sp3	Quintanar de la Sierra 1470	Peñalba (1994), Peñalba et al. (1996)	
sp4	La Paul de Bubal 1115	Jalut et al. (1992)	
sp5	Lago Banyoles 173	Pérez-Obiol and Julià (1994)	
sp6	Padul 785	Pons and Reille (1988)	
Italy			
it1	Lago di Montecchio 656	Watts et al. (1996)	
Germany			
g1*	N Schleswig Holstein	Usinger (1981), Usinger and Wolf (1982), Bock et al. (1985), Menke (1968)	
g2*	E Frisia	Behre (1966), Heider (1995), Mecke (1995)	
g3*	Mecklenburg-Vorpommern	Lange et al., (1986), de Klerk (1998)	
g4*	Berlin area	Brande (1980), Böse et al. (1995)	
g5	Schünebusch	Caspers (1993)	
g6	Asscherslebener See 238	Müller (1953)	
g7	Hünxe	Rehagen (1964)	
g8	Luttersee 165/Lüderholz 228	Chen (1988)	
g9	Krumpa 160	Litt (1994)	
g10	Oppershofen 141	Bos (1998)	
g11	Großes Moor 293	Streitz (1980, 1984)	

(continued on next page)

Table 3 (*continued*)

CODE		Refs.	
Germany			
g12 *	N. Bavaria	Hahne (1991)	
g13	Meerfelder Maar 334	Usinger (1982)	
g14	Fichtelberg 625	Hahne (1992)	
g15	Stürzer Lohe 420	Stalling (1987)	
g16	Kulzer moos 479	Knipping (1989)	
g17	Dösingerried 715	Stalling (1987)	
g18	Sims see 472	Beug (1976)	
g19	Reicher Moos 670	Bertsch (1961)	
Switzerland			
Sw1 *	Swiss Jura	Wegmüller (1977), Magny et al. (1998)	
Sw2 *	Swiss Plateau	Lotter (1988), Ammann (1989) Wegmüller and Lotter (1990), Wegmüller (1997/8)	
Sw3	Nussbaumer See 434	Rösch (1985)	
Austria			
a2	Lanser See 840	Bortenschlager (1984)	
a3	Lengholz 570	Fritz (1965)	
Hungary			
hu1	Dunakeszi	Járai-Komlódi (1968)	
Czech Republic			
cz1 *	Trebon Basin/S. Bohemia	Rybníckoví (1974), Jankovska (1980)	EPD
Poland			
p1	L. Druzno	Zachowicz et al. (1982)	
p2	Woryty 105	Pawlikowski et al. (1982)	
p3	Maly Suszek 115	Miotk-Szpiganowicz (1992)	
p4	L. Mikolajki	Ralska-Jasiewiczowa (1966)	
p5	L. Steklin	Noryskiewicz (1982)	
p6	L. Bledowo	Binka et al. (1991)	
p7	L. Gosciaz	Ralska-Jasiewiczowa et al. (1992)	
p8	Dziekanowicze 100	Litt (1988)	
p9	Zabinko	Bohncke et al. (1995)	
p10	L. Lukcze	Balaga (1990)	
p11	L. Perespilno 165	Goslar et al. (1999)	
p12	L. Slopiec	Szczepanek (1982)	
p13	Swilcza 220	Koperowa (1962)	
p14	Podbukowina 230	Koperowa (1962)	
p15	Na Grelu	Koperowa (1961)	
p16	Tarnawa Wyzna 670	Ralska-Jasiewiczowa (1980)	
Bulgaria			
Bu1	Kupena 1300	Huttunen et al. (1992)	EPD

b1*: W Belgium: Snellegem; Vinderhoute; Moerbeke; cz1*: Trebon Basin/S. Bohemia: Velanska Cesta (505), Cervene Blato (470), Barbora (435) Borkovicka Blata (407), Blato (645); f10*: Bas-Dauphiné: T. de Chirens (460), St. Julien de Ratz (650), Le Grand Lemps (500), Hières sur Amby (212), Loras (410); f11*: Haute Provence: Lac Long Inferieur (2090), Vallon de Provence (2075), Col des Lauzes (1784); f14*: France Eastern Pyrenées: La Borde (1660) , Lac Balcère (1764), Freychinède (1350); g1*: N Schleswig Holstein: Blixmoor, Glüsing, Wildes Moor, Esinger Moor; g2*: E Frisia: Vögelspohl, Westrauderfehn, Esinger moor, Deinstedt, Scharnhagener Moor; g3*: Mecklenburg-Vorpommern: Hoher Birkengraben; Tetel.; g4*: Berlin area: Ferch: Pechsee: Leckerpfhul.; g12*: N. Bavaria: Schwarzes Moor (781) Rappershausen (383); n1*: SW Norway: Sandvikvatn (128), Liastemmen; Eigebakken (270); sw1*: Swiss Jura. T. de Coinsins (480), Le Locle (915); sw2*: Swiss plateau. Rotsee (420), Lobsigensee (514), Aegelsee (995); Langnau (679); uk1*: Orkney Islands: Yesnaby, Little Lochans.; uk8* NE England Thorpe Bulmer, Seamer Carrs; Star Carr.

means of 10 simulated years, as we discarded the first two years to account for model spin-up. To make a meaningful model-data comparison, we converted both simulated and reconstructed temperatures to sea level, using a lapse rate of 6°C/km. It should be noted that for Europe the interannual variability in the model is typically 1°C for summer and 3°C for winter. Consequently, small simulated temperature anomalies (i.e. GI-1e–GS-2a or PB–GS-1) could be due to this variability instead of differences in boundary conditions.

3. Results

3.1. 14.7 k Transition

3.1.1. Simulation results

3.1.1.1. expGS-2a. The simulation results for the GS-2a climate suggest marked differences between July and January situations (Fig. 4a and b). In expGS-2a July temperatures range from 0°C in N Scandinavia and Scotland to 20–25°C in Spain (Fig. 4a). A strong N–S thermal gradient of 10°C within 5° of latitude is visible at 55–57°N around the ice-edge margin. The January results for expGS-2a suggest values ranging from −35°C over northernmost Scandinavia, to −15°C at 50°N and 0°C to 10°C over the Mediterranean (Fig. 4b).

3.1.1.2. expGI-1e. As expected, the maps for expGI-1e show a considerably warmer climate than that of expGS-2a. July temperatures vary from 5°C in the North of the study area to over 20°C over most of the European continent south of about 52°N (Fig. 4c). South of the Scandinavian Ice Sheet a strong N–S thermal gradient is present similar to expGS-2a. In the map for the January temperatures a NE to SW gradient is visible, with temperatures ranging from lower than −20°C in Finland to over 10°C in S Spain (Fig. 4d).

3.1.1.3. expGI-1e–expGS-2a anomaly. The simulated July temperature difference between expGI-1e and expGS-2a shows a warming ranging from 10°C over S Sweden to 2°C in NW Russia (Fig. 4e). Over most of the European continent a temperature increase of 4°C to 6°C is simulated, although this value is slightly higher near the Atlantic coast (i.e. 6°C to 8°C over Britain, Ireland and NW France). The expGI-1e minus expGS-2a result for the January temperatures reveals a strong west-to-east gradient at 55°N, varying from 25°C over Ireland to 5°C to 10°C over eastern Europe (Fig. 4f). This temperature rise is smaller in Southern Europe, with a difference of 5°C around the Mediterranean Sea. The mean annual effective precipitation increases over most of Europe in expGI-1e compared to expGS-2a (see Fig. 5). However, the increases are small, i.e. below 0.5 mm/day except for Sweden, Norway and Scotland where the values are higher.

3.1.2. Reconstruction results

3.1.2.1. GS-2a. The distribution of climate indicator plant-species suggests that GS-2a July temperatures ranged from values below 11°C north of 53/54°N to at least 15°C in S Europe, south of 44°N (Fig. 6a). The most important indicator species for GS-2a is *Hippophaë rhamnoïdes*, which requires July temperatures of at least 11°C to 12°C for reproduction (Fassl, 1996; Zagwijn, unpublished). Pollen grains of this species have been found throughout the study area, including sites above 500 m in central Europe, indicating 13°C to 15°C. A value of at least 16°C may be inferred for S Spain (Pons and Reille, 1988). Moreover, the presence of pollen of *Myriophyllum spicatum/verticilatum*, *M. alterniflorum* and *Juniperus* suggests temperatures between 9 and 11°C in the ice-free NW part of the study area. Occasional grains of *Nymphaea* in Wales (Walker, 1982) imply occasionally higher values during GS-2a. Pollen grains of *Fagus sylvatica* suggest that July temperatures reached 18°C in S Italy (Watts et al., 1996).

Periglacial evidence attributed to GS-2a indicates that maximum mean *annual* temperatures in NW Europe ranged from −8°C north of 54°N to below −2°C south of 50°N (Fig. 6b). Huijzer and Vandenberghe (1998) suggested the existence of continuous permafrost in a small zone near the ice front. Ice-wedge casts and fossil sand wedges in coarse sediments, indicating mean annual temperatures below −8°C to −6°C (Péwé, 1966; cf. Huijzer and Isarin, 1997), have been described for Ireland (e.g. Lewis, 1977), Wales (e.g. John, 1973), Scotland (e.g. Greig,

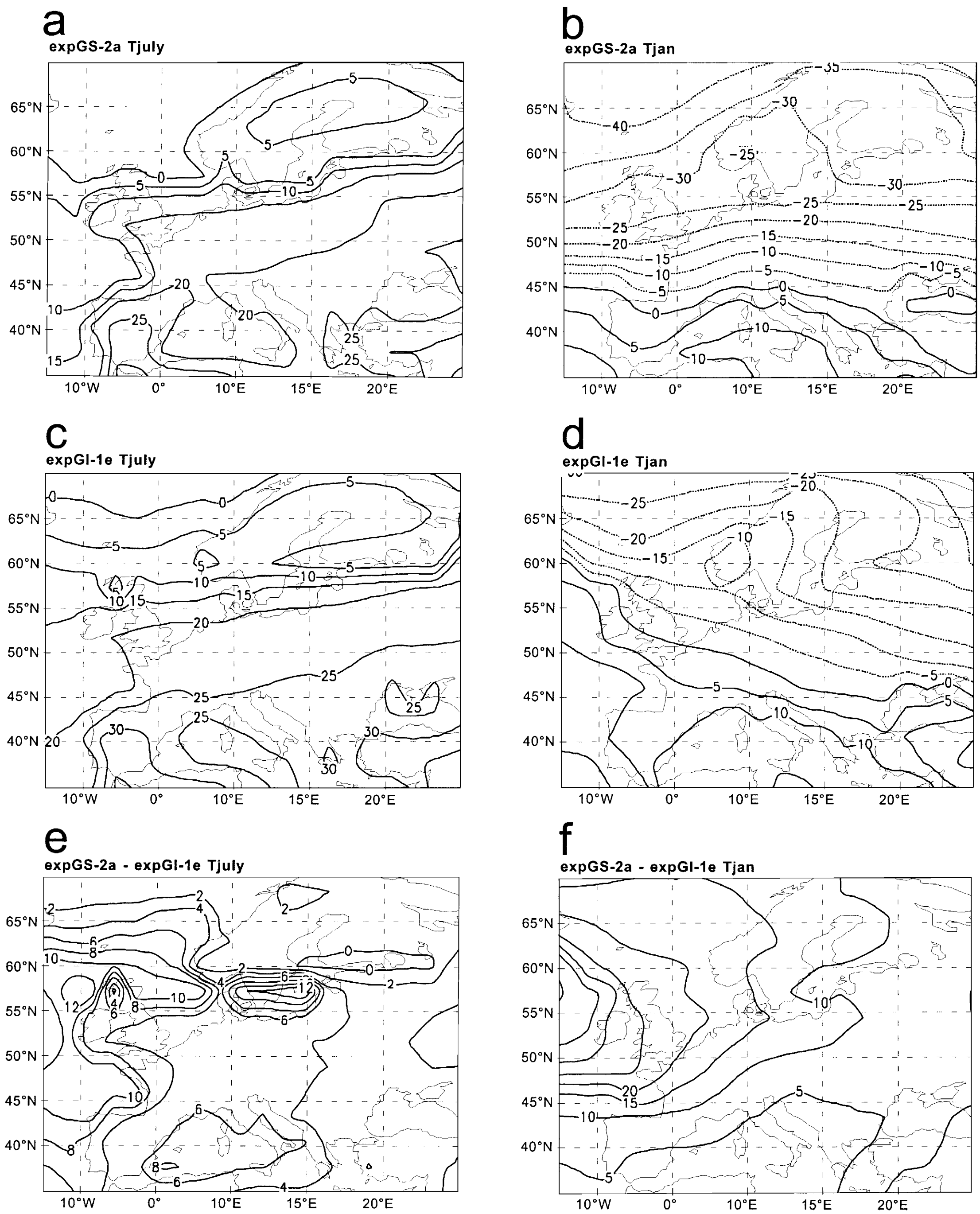

Fig. 4. Simulated mean January and July temperatures (in °C) at sea level: (a) July expGS-2a, (b) January expGS-2a, (c) July expGI-1e, (d) January expGI-1e, (e) July expGI-1e minus expGS-2a difference. (f) January expGI-1e minus expGS-2a difference. Contour interval in all figures is 5°C, except for (e) (2°C interval).

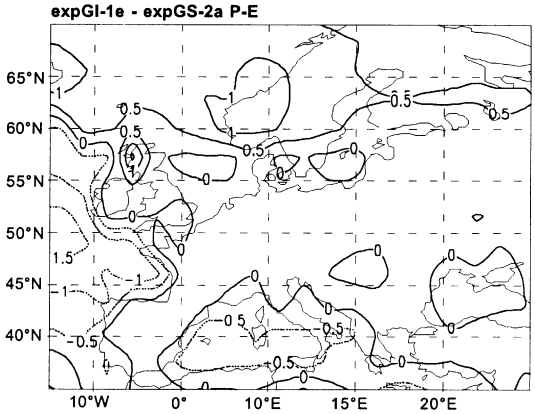

Fig. 5. Mean annual P-E (mm/day) difference between expGI-1e and expGS-2a. Contour interval is 0.5 mm/day.

1981), Denmark (e.g. Kolstrup and Mejdahl, 1986) and N Poland (e.g. Kozarski, 1993; Goździk, 1995). Wedge casts in fine-grained deposits, indicating a mean annual temperature below −4°C (e.g. Burn, 1990), have been observed in till in Wales (Saunders, 1973), N and central Poland (Goździk, 1986) and N Germany (Liedtke, 1957–1958) and in loess profiles in S Poland (Dwucet and Sniesko, 1996), Germany (Liedtke, 1957–1958) and W France (Helluin et al., 1977; Lautridou, 1985). Data from The Netherlands and Belgium consist primarily of seasonal frost cracks, suggesting mean annual temperatures below −1°C (e.g. Vandenberghe and Pissart, 1993). The absence of larger thermal contraction cracks in these areas, in either coarse or fine material, suggests that annual temperatures were higher than −4°C.

Fig. 6b also shows that GS-2a *January* temperatures may have been between −25°C and −15°C in NW Europe. Huijzer and Vandenberghe (1998) reconstructed maximum January values of −20°C for this region from ice-wedge casts and other types of large scale thermal contraction cracks. Further refinement of the temperature distribution in Europe based on this data source is difficult since the −20°C indicator value is a threshold value and large thermal contraction features are widespread throughout the study area. Alternatively, we calculated maximum January temperatures from reconstructed July (pollen, insects) and annual temperatures (periglacial), hereby assuming a sine temperature function. As a result, a tentative January temperature of −26°C may be calculated for the area north of 55°N (T_{july} above 10°C and T_{annual} below −8°C, resp.). Similarly, for the Netherlands, N Germany and N Poland (∼53°N) a January temperature below −20°C may be calculated, whereas for central France a value of −15°C was calculated. The situation south of 47°N is unclear due to the absence of periglacial and botanical evidence.

3.1.2.2. GI-1e. Palaeobotanical evidence indicates that GI-1e July temperatures ranged from below 13°C at 54°N to over 20°C in the Iberian Peninsula (Fig. 6c). The temperatures of 11 to 12°C in ice-free Scandinavia are based on finds of *Sanguisorba minor*, and *H. rhamnoïdes* (Iversen, 1954; Bjelm, 1976). Similarly, *Typha latifolia* grains suggest values of at least 13°C to 15°C for Ireland (Andrieu et al., 1993, p. 695) and Wales (Walker and Harkness, 1990). July temperatures of at least 16°C are inferred for central Europe based on observations of *T. latifolia* pollen in Switzerland (Ammann, 1989) and S Germany (Beug, 1976), *Najas marina* pollen in Poland (Bałaga, 1990) and spines of *Ceratophyllum* sp. in central Germany (Bos, 1998). Even temperatures above 18°C are deduced for Switzerland based on finds of *T. latifolia* and *S. minor* (Wegmüller and Lotter, 1990). Following Kolstrup (1980), the finds of *Polygonum viviparum* pollen at another site in Switzerland (Lobsigensee; Ammann, 1989) may indicate that T_{july} did not exceed 21°C. A July temperature of 21°C is inferred for Portugal based on observed *S. minor* pollen (Van der Knaap and Van Leeuwen, 1997), whereas in S Spain pollen of *Quercus suber* (Pons and Reille, 1988), indicative for minimum July values of 19°C (Fassl, 1996), suggest that temperatures exceeded 23°C.

The combination of periglacial, beetle and pollen evidence suggests that during GI-1e *January* temperatures probably ranged from 6°C in Spain to well below 0°C in NW Europe (Fig. 6d). Reconstruction of January isotherms for GI-1e is not feasible due to the limited number of sites and the absence of periglacial evidence. The latter may suggest that mean annual temperatures were above −1°C to 0°C in the study area. However, in areas close to the receding ice front January temperatures may have been low enough to induce periglacial activity (see discussion e.g. in Ballantyne and Harris, 1994). The

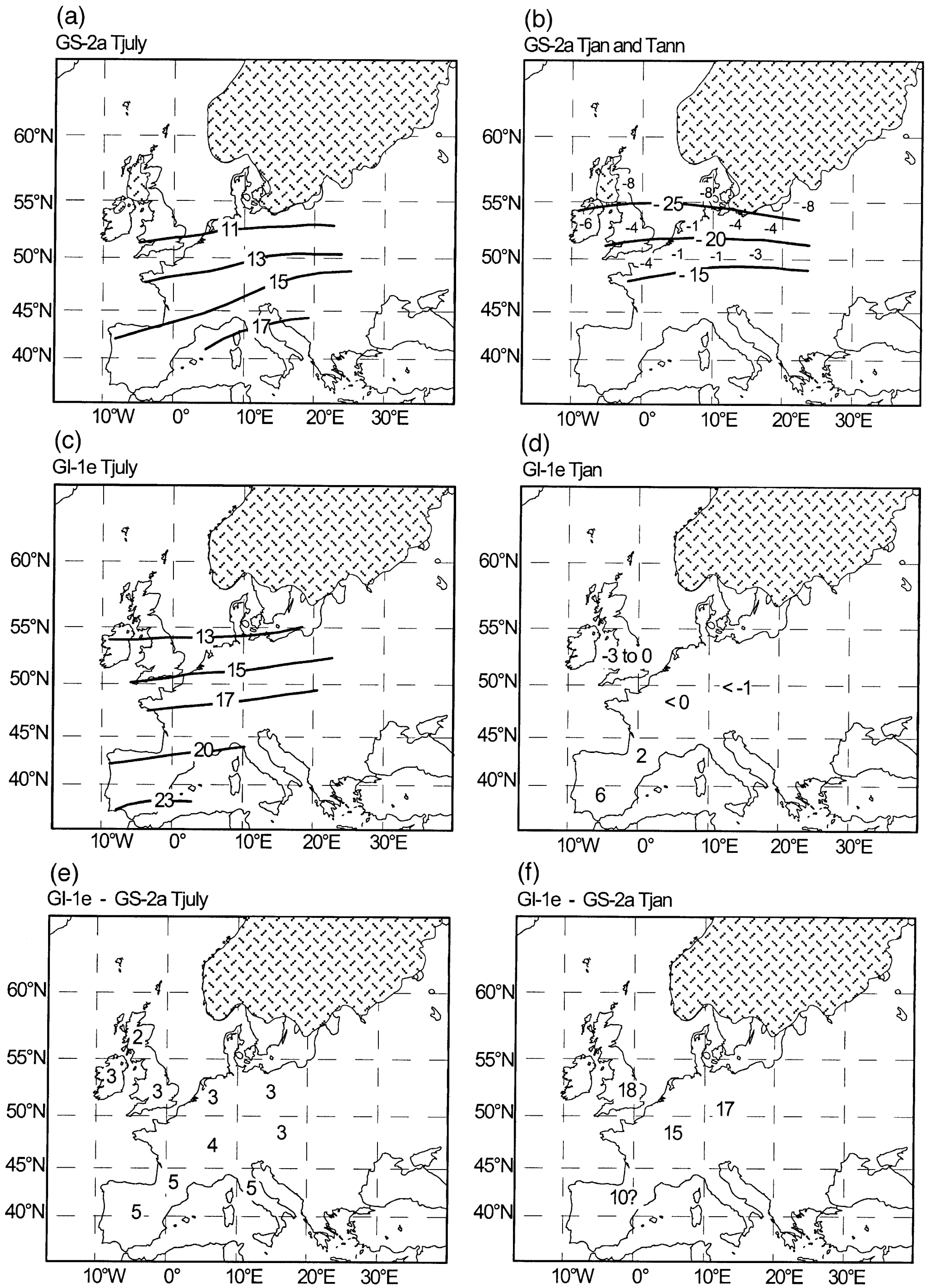

Fig. 6. Reconstructed mean July and January temperatures (in °C) at sea-level: (a) July GS-2a, (b) January GS-2a (isotherms) and annual (point values), (c) July GI-1e, (d) January GI-1e, (e) July GI-1e minus GS-2a difference. (f) January GI-1e minus GS-2a difference. See Table 2 for data sets used for the reconstruction.

presence of casts of syngenetic ice-wedges in outwash sediments in e.g. Denmark (Habbe, 1993) may suggest that (at least occasionally) thermal cracking did occur with associated temperatures below −15°C to −20°C during GI-1e. Paleobotanical evidence points to January temperatures well above 0°C in the Iberian Peninsula, as *Q. suber* was found at Padul (Pons and Reille, 1988) and *Q. ilex* at Banyoles (Pérez-Obiol and Julia, 1994). A local January temperature of below −2°C is inferred for S Poland based on pollen of *Pleurospermum austriacum* (Iversen, 1954; Koperowa, 1962). The reconstructed pattern agrees with beetle evidence that suggests mean temperatures of the coldest month in Britain in the order of −3°C to 0°C (Lowe et al., 1999). There are some indications that in GI-1e seasonal frost occurred regularly, for instance the observation of fragipans and illuvation in loess soils in France by Van Vliet-Lanoe et al. (1992) and noted changes in fluvial geomorphology in NW Europe suggesting melting of thick snow packs (Vandenberghe et al., 1994).

3.1.2.3. GI-1e–GS-2a anomaly. Fig. 6e and f show the anomaly maps resulting from subtraction of the GS-1e and GS-2a July and January situations. For July a N–S gradient is visible, varying from 2°C near the ice front to 5°C south of 45°N. The sparse data on the January situation suggest that January temperatures increased by at least 15°C in a large part of Europe (Fig. 6f). For the January temperatures in the Iberian Peninsula a tentative increase of 10°C is inferred, which is based on an extrapolation of the January isotherms in Fig. 6b.

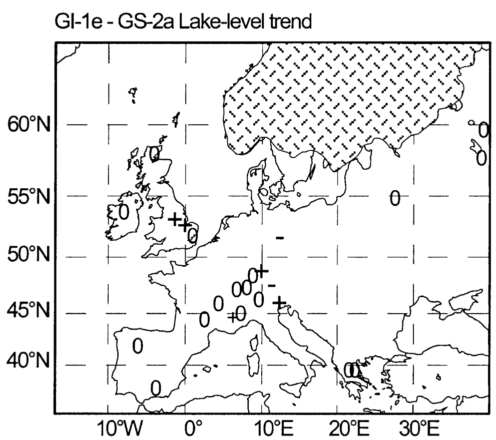

Fig. 7. Reconstructed lake level trends during the 14.7 k transition, based on Lake Status Data Base of Yu and Harrison (1995) and Tarasov et al. (1996).

The mapping of changes in lake level status (Fig. 7) suggests that effective precipitation remained the same with a possible increase in SE England, SE France and south-central Europe. An increase of precipitation is supported by fluvial data from NW Europe, showing dramatic enhancement of fluvial activity during the transition from GS-2a to GI-1e (Vandenberghe et al., 1994; Huisink, 2000). Zazo et al. (1996) suggested that during GI-1e, karst activity in Spain increased due to an increase of effective precipitation. The latter observation is not reflected in the (scarce) lake level data from this area.

3.2. 11.5 k Transition

3.2.1. Simulation results

3.2.1.1. expGS-1. The results of expGS-1 show a strong N–S temperature gradient for both July and January. The model produces mean July temperatures varying from below 5°C in N Europe, to 15°C at 50°N and over 20°C in S Europe (see Fig. 8a). The simulated January temperatures are below −20°C in N Scandinavia, and increase towards values of −5°C at 50°N and over 5°C in Spain (Fig. 8b). This pattern is different for Ireland and Britain, where the model produces higher January temperatures compared to the same latitudes at the continent (between 0°C and −10°C).

3.2.1.2. expPB. The calculated PB-climate is the warmest of the four simulated palaeoclimates. The July temperatures reach values of more than 15°C over most of Europe, except were land ice is present (Fig. 8c). During January a clear E–W thermal gradient is visible that is similar to that of today, with temperatures increasing from −15°C in Russia to over 5°C in Ireland (Fig. 8d).

3.2.1.3. expPB–expGS-1 anomaly. The July temperature rise increases in a northward direction from 2°C in Spain to 8°C at 55°N (Fig. 8e). In S Sweden a strong reverse gradient is present from 12°C at 57°N to 0°C at 60°N. The expPB–expGS-1 anomalies for

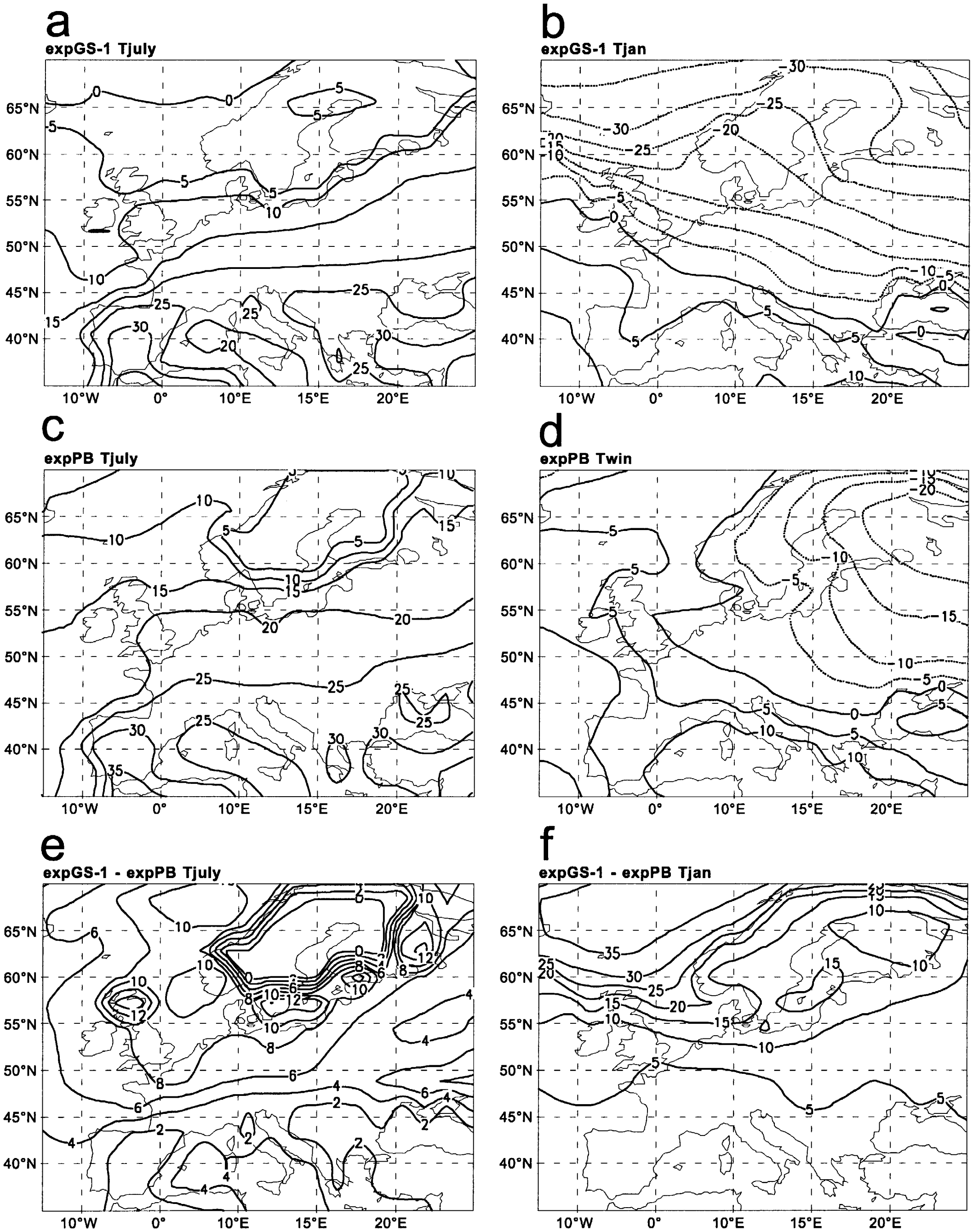

Fig. 8. Simulated mean January and July temperatures (in °C) at sea level: (a) July expGS-1, (b) January expGS-1, (c): July expPB, (d): January expPB, (e) July expPB minus expGS-1 difference. (f) January expPB minus expGS-1 difference. Contour interval in all figures is 5°C, except for (e) (2°C interval).

January show a strong warming over N Europe (more than 10°C) that rapidly declines towards the South with values less than 5°C south of 50°N (Fig. 8f). The P-E result for expPB minus expGS-1 shows a patchy pattern with some regions with increases surrounded with areas where the effective precipitation decreased (Fig. 9).

3.2.2. Reconstruction results

3.2.2.1. GS-1. During GS-1, mean July temperatures ranged from ~10°C north of 56°N, e.g. in ice-free Sweden and Scotland, to well above 20°C at the Iberian Peninsula (Fig. 10a). Isarin and Bohncke (1999) reconstructed temperatures of 10°C to 15°C for NW Europe during the first and coldest part of GS-1. Additional data are broadly in accordance with this reconstruction. A mean July temperature of more than 18°C is indicated by pollen of *S. minor* and *Hippophaë* at high altitude sites in S France (e.g. La Paul de Bubal: Jalut et al., 1992), and by botanical evidence (wood fragments of *Buxus sempervirens* and *Acer monspessulanum*) from prehistoric hearths in S France (Heinz and Thiébault, 1998; Fassl, 1996). Pollen of *S. minor*, observed in Portugal (Van der Knaap and Van Leeuwen, 1997), suggest that July temperature were near 21°C.

Reconstructions of both January and annual temperatures for NW Europe during the coldest part of GS-1 have been described by Isarin (1997) and Isarin et al. (1998). These reconstructions, primarily based on periglacial data, indicate values similar to the GS-2a situation, with a T_{jan} ranging from −25°C at 55°N to −15°C at 50°N (Fig. 10b). The burned wood fragments of *Buxus* and *Acer* observed by Heinz and Thiébault (1998) and mentioned above may indicate that T_{jan} was near or above 0°C in S France.

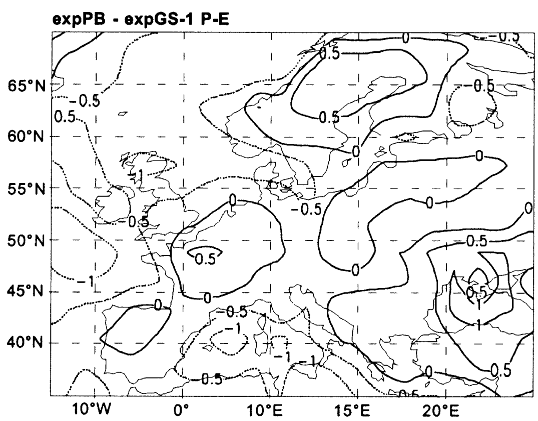

Fig. 9. Mean annual P-E (mm/day) difference between expPB and expGS-1. Contour interval is 0.5 mm/day.

3.2.2.2. PB. The reconstructions suggest that PB July temperatures ranged from at least 13°C north of 55°N to 23°C at 40°N (Fig. 10c). The values in the north of the study area are based on finds of *T. latifolia*, *Cladium mariscus*, *Thelypteris palustris* and *Ceratophyllum demersum*, indicating July temperatures of around 16°C in S Sweden (Åkerhultagöl, B. Berglund, EPD data), Ireland (Watts, 1977) and Germany (e.g. Stalling, 1987; Hahne, 1991; Bos, 1998). In SE France (Hières-sur-Amby) a July temperature of at least 17 to 18°C is inferred from the presence of *Q. ilex* (Clerc, 1988), whereas values well above 20°C are suggested for Spain based on finds of *Q. suber* and *Q. ilex* (Pons and Reille, 1988; Pérez-Obiol and Julia, 1994). In addition, finds of *N. marina* indicates values of at least 19°C in Italy (Watts et al., 1996). The presence of *T. latifolia* in Portugal (Van der Knaap and Van Leeuwen, 1997) and Bulgaria (Huttunen et al., 1992) points at temperatures of at least 21°C.

The PB January temperatures range from +5°C in the southern part to below zero in the northern part of the study area (Fig. 10d). The results are partly based on Zagwijn (1994), who inferred January temperatures above −2°C to −6°C in the British Isles, Ireland, S Sweden and N Poland based on the presence of *Corylus avellana* around 9500 BP (see Zagwijn's Fig. 3). Additional data are in accordance with Zagwijn's reconstruction. January temperatures below +0.5°C to 1.5°C are suggested by finds of *P. austriacum* pollen in the Czech republic (Rybnickova, 1974) and Poland (Koperowa, 1962). Moreover, in southern France values of +2°C to +3°C are indicated by finds of *Q. ilex* pollen (Hières-sur-Amby and Grand Lemps: Clerc, 1988) and wood fragments of *B. sempervirens* and *Q. ilex/coccifera* in prehistoric hearths (Heinz and Thiébault, 1998). Similarly, in Spain a January temperature of +2 to +5°C is suggested by pollen of *B. sempervirens* (Pérez-Obiol and Julia, 1994) and of *Q. suber/Q. ilex* (Pons and Reille, 1988).

3.2.2.3. PB–GS-1 anomaly. The T_{july} anomaly map (Fig. 10e) shows that PB July temperatures increased

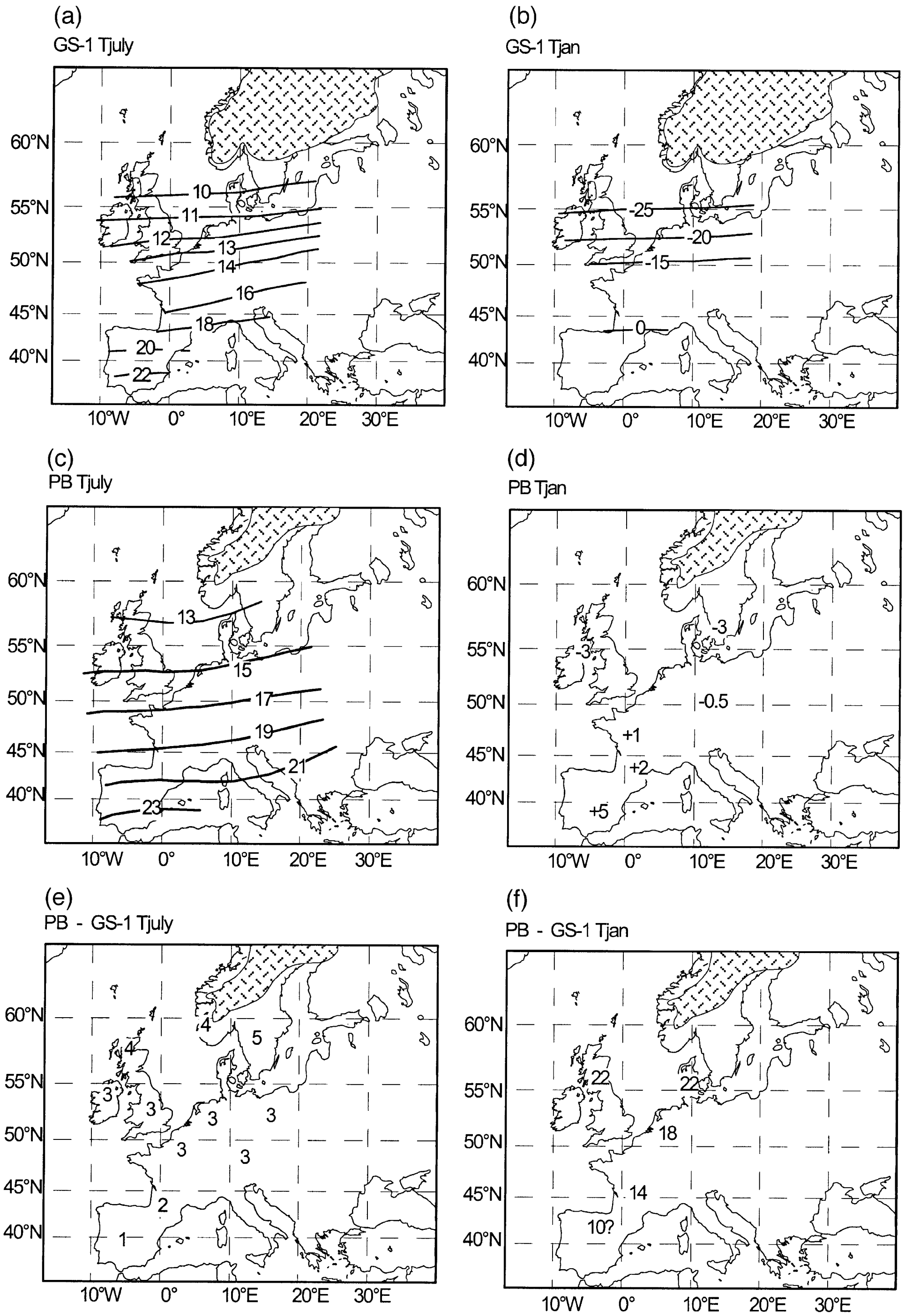

Fig. 10. Reconstructed mean July and January temperatures (in °C) at sea-level: (a) July GS-1, (b) January and annual GS-1, (c) July PB, (d) January PB, (e) July PB minus GS-1 difference. (f) January PB minus GS-1 difference.

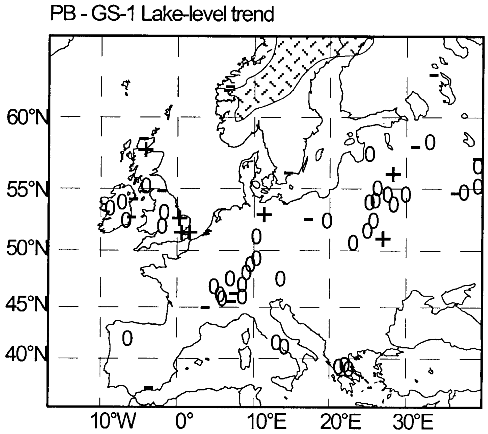

Fig. 11. Reconstructed lake level trends during the 11.5 k transition, based on Lake Status Data Base of Yu and Harrison (1995) and Tarasov et al. (1996).

by at least 4 to 5°C north of 55°N when compared to GS-1. A value of at least 3°C is inferred for NW and Central Europe. South of 45°N, the temperature increase is limited to 1 to 2°C. The reconstructions show that January temperatures increased dramatically during the 11.5 k transition with values of at least 15°C (Fig. 10f).

The lake level trends for the 11.5 k transition suggest a large regional diversity (Fig. 11). For example, in the British Isles a zone of falling and of rising lake levels may be discerned. Data from the Baltic states indicate stable and rising lake levels. Stable or falling lake levels have been reconstructed for the Mediterranean and south central Europe. Valero-Garcés et al. (1998) reconstructed low lake levels during the final part of GS-1 and a significant increase during PB for the western Mediterranean region. These observations are in agreement with lake-level data from the Jura mountains (Magny and Ruffaldi, 1995).

4. Discussion

In the following sections we discuss the comparison of the presented AGCM results and climate reconstructions. It should be noted that such a comparison involves three factors of uncertainty (c.f. Isarin and Renssen, 1999). These factors are (1) the model performance, (2) the set of boundary conditions and (3) the climate reconstruction. Considering the realistic modern climate that is produced by ECHAM4 (c.f. Roeckner et al., 1996), and the uncertainties that are involved when working with palaeodata (c.f. Isarin and Renssen, 1999), it may be assumed that uncertainties in the model performance are less significant than the other two factors.

4.1. 14.7 k Transition

4.1.1. GS-2a temperatures

The model and reconstructions produced similar GS-2a July temperatures north of ~52°N, with values between 15°C and 0°C (compare Figs. 4a and 6a). Our pollen-based estimates are comparable with those based on beetle data of Coope et al. (1998). South of this latitude the model suggests slightly higher temperatures (2°C to 3°C difference with reconstructions), with values over 15°C over most of France. The strong N–S gradient at ~ 55°N (i.e. 5–10°C within ~100 km) noted in Fig. 4a seems to be realistic. This feature is related to the strong contrast in thermal properties between the ice sheets and the sea ice on the one hand and the bare land surfaces—warmed by the relatively strong summer insolation—on the other hand. The model may have reacted too strongly to this summer insolation, as suggested by the higher July temperatures in S Europe in the simulation compared to the reconstruction.

Considering GS-2a January temperatures, the reconstructed −25°C and −20°C isotherms are more or less reproduced by the model (see Figs. 4b and 6b). South of 50°N the model is a few degrees warmer than the reconstruction. However, the absence of data prohibits a direct model–data comparison for the area south of 45°N. It should be noted that calculation of January temperatures using July and annual values may produce too cold estimates (by ~4°C, see Isarin et al., 1998). Moreover, time-control of some of the periglacial data used for the annual and January temperature reconstructions is rather poor (Huijzer and Vandenberghe, 1998). This may imply that these features represent earlier and colder phases like the LGM. Taking these uncertainties into account, we propose that the model simulated reliable GS-2a January temperatures. In the simulation the low temperatures in Europe are the result of the strong cooling of air over the extended Atlantic sea ice cover. The good model–data fit suggests that the boundary conditions we prescribed for expGS-2a, including the CLIMAP SSTs, are appropriate.

4.1.2. GI-1e temperatures

The simulated GI-1e July temperatures are about 5°C higher than the reconstructed values (Figs. 4c and 6c). It should be realised that the pollen-based estimates are minimal values. Still, the differences are too large to be explained by this artefact of the method. However, it is interesting to note that the model–data match is better when Fig. 4c is compared with the beetle-based temperature reconstruction of Coope et al. (1998), as the latter study suggests local values of 17–21°C between ~50°N and ~55°N. On the other hand, in earlier studies we have shown that the model tends to produce too warm conditions under influence of the high insolation (Renssen and Isarin, 1998). Renssen et al. (2000) showed that permafrost may play a role in depressing stadial July temperatures. However, during GI-1e permafrost was presumably restricted to a narrow zone along the ice margin. In summary, we propose that the ‘true’ GI-1e July temperatures have been intermediate between our simulated and reconstructed values (i.e. close to the beetle data).

The model and reconstruction remarkably produce similar GI-1e January temperatures, with a NE-to-SW temperature gradient with values ranging from below 0°C in Britain and NE France, to over 5°C in the Iberian Peninsula (see Figs. 4d and 6d). As mentioned before, the reconstruction is based on a limited data set. Therefore, we are not able to make decisive conclusions on the validity of both the simulated and reconstructed GI-1e January temperatures.

4.1.3. GI-1e–GS-2a temperature anomalies

For the July conditions in continental Europe south of ~50°N there is agreement between model results and reconstructions as both show a warming of about 5°C (compare Figs. 4e and 6e). This increase of ‘only’ 5°C indicates that the assumed strong warming of the Atlantic Ocean (~10°C, compare Fig. 2e and g) is not the most important driving factor for the July temperature distribution on the European continent. Further north the model suggests a stronger warming than the reconstruction, especially in those regions that became ice-free during GI-1e. For instance, the simulation suggests a strong increase of 10°C for S Sweden, a region deglaciated during the GI-1e–GS-2a transition. Obviously, no reconstructed estimate for the temperature increase could be obtained for regions that are glaciated during GS-2a. However, the simulated value of 10C is in agreement with beetle-based estimates of 7°C to 12°C in NW Europe.

The few data points that give information on the GI-1e minus GS-2a January temperature anomalies show the same pattern as in the model result (see Figs. 4f and 6f). A contrast between N and S Europe is noted, with the largest warming over Britain and a smaller effect to the South. The model suggests that the maximum anomaly—over 25°C—was present over Ireland. Moreover, the simulation indicates the existence of a clear E–W gradient, as the anomaly only is 5°C to 10°C at the same latitude (55°N) in Russia. The latter gradient is not seen in the data, presumably due to the limited number of sites. The pattern seen in the simulation is caused by the change in ocean surface conditions over the GI-1e–GS-2a transition. We assumed a shift in the winter sea ice margin from 47°N in expGS2-a to 60°N in expGI-1e, associated with an inflow of relatively warm waters along the European coast (compare Fig. 2f and h).

4.1.4. GI-1e–GS-2a mean annual P-E anomalies

Both simulation and reconstruction indicate that few changes in P-E occurred during the GS-2a to GI-1e transition over the continent. The model produced a small increase of less than 0.3 mm/d in over C Europe (not shown). The exceptions are N Scandinavia north of ~60°N, where P-E increases by up to 1 mm/day according to the simulation, and the Atlantic ocean, where P-E decreases. The latter changes can be explained by considering the regional differences in precipitation and evaporation.

In the simulation results the precipitation increases everywhere in Europe in expGI-1e compared to expGS-2a, but most distinctly north of the line Scotland–Denmark (not shown). The general increase can be related to the prevailing rule that warm air is more humid than cooler air (i.e. it has a greater vapour holding capacity). The relative strong increase in the North of the study area, however, is likely to be related to the northward shift of the sea ice margin and the oceanic polar front during the GS-2a–GI-1e transition. Assuming that the used SST-sets for our experiments are realistic, the sea ice margin shifted from a winter position at ~47°N during GS-2a to ~60°N in GI-1e (see Fig. 2f and h).

The effect of this northward shift on the atmospheric winter circulation is shown in Fig. 12a and b. In expGS-2a the atmosphere is stabilized north of 50°N due to the strong surface cooling over the extended sea ice cover (Fig. 12a), resulting in a relative high sea level pressure. In contrast, in expGI-1e a clear Icelandic Low is present, producing a strong pressure gradient over NW Europe, which was accompanied with a strong increase of cyclonic activity in northern Europe. Modelling studies show that the main storm track follows the sea ice margin (Valdes and Hall, 1994; Renssen et al., 1996; Kageyama et al., 1999). Thus, the storm track followed the northward shift of the sea ice margin and moreover, the N Atlantic between 47°N and 60°N became available as a moisture source. Consequently, a relatively strong precipitation increase in N Europe follows. When comparing the evaporation figures for expGI-1e and expGS-2a, the values increase also over most of the study area, especially over the relatively warm ocean waters (not shown) where the increase is larger than the precipitation increase (note negative P-E anomaly in Fig. 5). The opposite occurs over N Europe, however, where the precipitation increase is larger than that of the evaporation, due to the relative cold conditions (restricting evaporation) that remain there in expGI-1e compared to W Europe.

4.2. 11.5 k Transition

4.2.1. GS-1 temperatures

The simulated GS-1 July temperatures are in agreement with the reconstructions north of 52°N. Here, both Figs. 8a and 10a suggest values between 15°C and 10°C. MCR estimates are in fair agreement with our pollen-based inferences (Coope et al., 1998). South of 52°N the model produces temperatures that are 3°C to 6°C higher than in the reconstruction. According to the model, July temperatures in Spain reached 30°C. How can we explain the model–data mismatch? In earlier studies, we already concluded that the used model tends to react in a very sensitive way to the high summer insolation. In Renssen and Isarin (1998) we concluded that the soil module of ECHAM4 might be too simplistic to realistically simulate the soil–atmosphere interaction under changed conditions. In the experiment shown here (i.e. expGS-1), we actually prescribed permafrost north of 50°N by introducing a simple parameterisation (see Table 1) to compensate for the supposed shortcomings of the model. This addition to the model produced much more realistic July temperatures for GS-1 compared to previously performed experiments without a permafrost parameterisation (see Renssen et al., 2000). Still, we cannot exclude that a deficiency in the model is causing the noted discrepancy between simulation and data for S Europe.

The model produced warmer GS-1 January conditions in NW Europe than indicated by the reconstruction (Figs. 8b and 10b), especially in Ireland and the British Isles. Here the reconstruction shows temperatures as low as −25°C to −20°C, whereas the model gives −15°C to 0°C in this region. The causes for this discrepancy have been thoroughly discussed in Renssen and Isarin (1998). In short, we argued that the model–data disagreement must have been caused by the ocean surface conditions prescribed in expGS-1. The winter sea ice margin must have been located at 52°N during GS-1 instead of at 60°N as we defined (see Fig. 2d). This is consistent with the finding of ice rafted sediments of GS-1 age near Portugal (Bond et al., 1993).

4.2.2. PB temperatures

The simulation again produces higher PB July temperatures than the reconstructions (2°C to 7°C difference, compare Figs 8c and 10c). The difference between both results increases to the South, with a maximum in the Iberian Peninsula. The model–data mismatch may have (partly) been caused by the prescribed SSTs in expPB. We assumed that the ocean surface conditions approached the modern ones during the PB. This assumption was in agreement with the SST reconstructions of Schulz (1995). However, it may be expected that the Atlantic Ocean was cooler than today, as there must have been a considerable influx of cold melt water originating from the remaining ice sheets. Still, the North-to-South increase in model–data difference cannot be explained by too warm Atlantic Ocean conditions in expPB, suggesting that other unknown factors may have played a role. Alternatively, the model–data mismatch can be partly attributed to an underestimation of the July temperatures by the reconstruction results shown in Fig. 10c. In analogy to the situation during GI-1e, the MCR estimates give a better match with the experimental results. Beetle evidence suggests July temperatures of 15–19°C north of 50°N.

A comparison of PB January temperatures (Fig. 8d and 10d) shows a general agreement between simulations and reconstructions. A similar SW–NE gradient is visible in both figures. The January temperatures are varying in both figures between 5–10°C in Spain and −5°C in S Scandinavia. An exception to this observation is the result for Ireland and Britain, where the model result (~ 5°C) is considerably warmer than the reconstruction (−3°C). The latter mismatch again suggests that we prescribed a

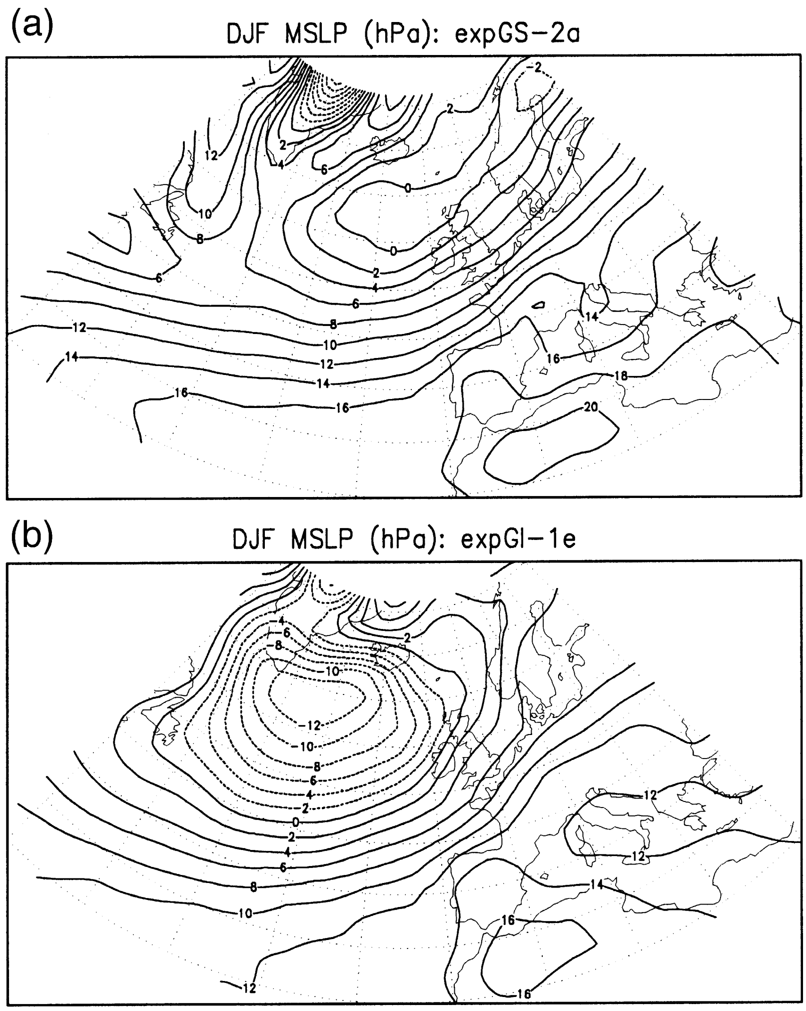

Fig. 12. Simulated mean sea level pressures for December–January–February (DJF) for experiments expGS-2a, expGI-1e, expGS-1 and expPB. Contour interval is 2 hPa. Values are given as deviations from the global DJF mean to account for the introduction of ice sheets.

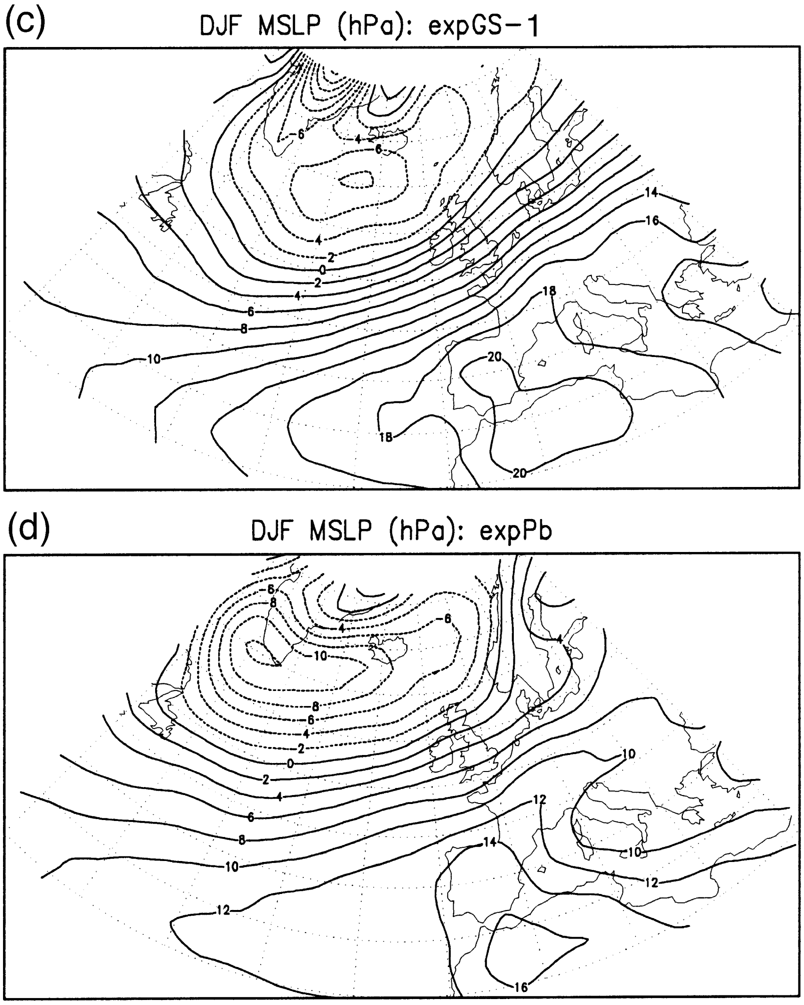

Fig. 12 (*continued*).

too warm N Atlantic Ocean in expPB (see previous paragraph). However, it should be noted that the number of sites used for the reconstruction of PB January temperatures is very limited.

4.2.3. PB–GS-1 temperature anomalies

The N–S July temperature anomaly gradient in both the reconstruction and the simulation result are alike, as in both Figs. 8e and 10e a minimal warming is seen in S Europe (less than 2°C), whereas the increase amounts up to 10°C in N Europe. The noted N–S gradient reflects partly the relatively strong effect of oceanic warming in N Europe. In the simulations we assumed that the Nordic seas were ice-free during PB, causing a relatively strong advection of heat to N Europe in expPB compared to expGI-1e (compare Figs. 4c and 8c). The strong temperature gradient over Scandinavia as visible in Fig. 8e is not reproduced in the reconstruction. This can be attributed to the obvious lack of data in the region covered by the ice sheet during the 11.5 k transition.

The N–S gradient is also seen in the PB minus GS-1 January temperature anomalies (Figs. 8f and 10f). As in the case of the 14.7 k transition, we attribute the strong increase during January to the influence of the Atlantic ocean. However, it should be noted that compared to the reconstruction, in the simulation result the gradient is shifted a few degrees of latitude to the North. This may be attributed to the position of the winter sea ice margin in expGS-1. As discussed above, this sea ice margin probably had a more southerly position during GS-1 than we prescribed in expGS-1, i.e. 5° of latitude, or 2 grid cells (e.g. Renssen and Isarin, 1998).

4.2.4. PB–GS-1 mean annual P-E anomaly

Two trends in P-E are clearly visible in both the simulation and the reconstruction: stable or slightly increasing P-E on the continent, decreasing along the coasts of the Nordic and Mediterranean seas, and Atlantic Ocean (see Figs. 9 and 11). How can we explain this pattern?

The processes that explain this pattern are similar to the GI-1e minus GS-2a anomaly discussed above. The AGCM results indicate that precipitation increases almost everywhere, especially in N Europe, where a northward shift of the main storm tracks is simulated. As seen in Fig. 12c and d, the main pressure gradient over northern Europe shifts northwards in expPB compared to expGS-1, leading to more frequent depressions in this region. Evaporation also increases over most surfaces, especially over the warmed surface waters. However, evaporation remains low over the Scandinavian ice sheet, caused by the prolonged cooling here. The latter explains the P-E increase over Scandinavia. A general increase in precipitation is expected during a transition from a cold to a warm climate and explains the positive P-E anomaly over the continent (see discussion on GS-2a–GI-1e transition). A second factor is that we prescribed an unlimited soil moisture supply in NW Europe in expGS-1 (cf. Renssen et al., 2000), causing relative high evaporation values in expGS-1. As a result, the evaporation in expPB is only slightly higher than in expGS-1 or even lower in some regions, thus producing a more positive P-E anomaly over the continent compared to the GI-1e minus GS-2a anomaly. Finally, it should be noted that there is evidence for a drier, second phase of the GS-1 (Walker, 1995). If valid, this would imply an even stronger positive anomaly over the 11.5 k transition.

4.3. Comparison of two transitions and climatological implications

A comparison of the two transition phases reveals some marked similarities and differences. The *similarities* can be summarised as follows: (1) the change in temperature generally increases going from S to NW Europe, (2) the increase in January temperature is much stronger than the increase in July temperature, (3) the change in 'effective' precipitation is not as marked as the change in temperature. The following *differences* between the 14.7 and 11.5 k phases may be identified: (1) the 11.5 k transition shows a warming during July in S Europe that is smaller than during the 14.7 k transition, (2) during the 11.5 k transition there is only a N–S gradient in the January temperature anomaly, whereas there is an additional W–E gradient in the 14.7 k shift. How can we explain these observations and what are the implications in terms of climate? Before answering these questions, it is necessary to consider the aspect of uncertainty.

The model–data comparison enabled us to draw conclusions on the three factors of uncertainty mentioned earlier, viz. (1) the model performance, (2) the boundary conditions and (3) the climate reconstruction. A short overview is given here. After clarifying the role of the three factors, we may infer the importance of the various driving factors behind the two climate transitions.

4.3.1. Model performance

We assumed that the model performance was of less importance than the other two factors, since the model is capable to simulate the present climate reasonably well (Roeckner et al., 1996, Pinot et al., 2000). Moreover, Kageyama et al. (1999) showed that the ECHAM model (in this case version 3) simulated more realistic storm tracks than other AGCMs. It should be realized that a good representation of the present climate does not prove that the model's sensitivity is correct. However, a recent study (Pinot et al., 2000) showed that, at least for the LGM climate, the ECHAM model performed within the range provided by other models. Our model–data comparison taught us that the ECHAM model tends to simulate anomalously high summer temperatures as a reaction to the relatively high summer insolation values. The simulation of relatively warm summer conditions over Europe is a known model bias (Roeckner et al., 1996). In the case of the climate of GS-1, we analysed the high summer temperatures in detail in earlier papers and inferred that the soil module of ECHAM4 may be too simplified to adequately deal with the changed radiation (Renssen and Isarin, 1998; Renssen et al., 2000).

4.3.2. Boundary conditions

The conditions in the N Atlantic Ocean are crucial to the model results and yet relatively uncertain. We inferred from the model-data comparison that the prescribed surface ocean conditions appear to be realistic for expGS-2a and expGI-1e. However, in expGS-1 the winter sea ice margin was positioned too far to the North, causing too warm January conditions close to the Atlantic coast (Renssen and Isarin, 1998). Moreover, we argued that the prescribed modern ocean conditions in expPB were unrealistic, implying that the Atlantic Ocean was a few degrees cooler during the PB than today. We have not found indications that other prescribed boundary conditions (i.e. ice sheets, vegetation parameters, greenhouse gasses, insolation) were unrealistic.

4.3.3. Climate reconstructions

We consider the reconstructions as reliable, since they are based on a combination of data sets, in total including more than 400 sites. Data within the individual data sets have been treated in standardised procedures. However, data are unevenly distributed throughout the study area: data sets for S and E Europe clearly need extension. Moreover, the reconstructions lack quantification of errors. Although, as mentioned in 2.2, insect- and pollen-based temperature estimates may both represent true mean values for stadial conditions, this appears not to be the case for relatively warm phases. The model–data comparison revealed that the simulated July temperatures for GI-1e and PB were in some instances in better agreement with temperature reconstructions based on beetles than with the pollen-based reconstructions. This observation could imply that beetles are better indicators for interstadial July temperatures than climate indicator plant species. However, as mentioned before, the reconstructions based on climate indicator plant species are *minimum* values. In addition, the number of plant species indicating July temperatures above 13°C is limited, which may partly explain the underestimation of July temperatures as compared to those based on beetle data. Based on various factors, Isarin and Bohncke (1999) estimated the uncertainty of their pollen-based temperature reconstructions at 1 to 2°C. Similarly, calculation of past January temperatures may include errors of several degrees Celsius (Isarin et al., 1998, p. 451). As described before, few data (and climate diagnostic features) are available for the reconstruction of GI-1e and PB January temperatures. Consequently, no isotherms could be reconstructed. A reliable proxy for former January temperatures is clearly needed.

4.3.4. Importance of various forcing factors

The presented results illustrate that the surface conditions in the Atlantic Ocean represent the most important factor driving the warming during the two transitions in Europe. In both cases, the increase in January temperature over NW Europe is much stronger than the increase in July temperature. The January temperature increase is governed by the position of the Atlantic sea ice margin. Over the extended sea ice cover the air is strongly cooled to temperatures below −30°C. Consequently, the sea ice cover is the source region of very cold air. We inferred that during GS-2a and GS-1 this winter sea ice margin was situated at mid-latitudes (~45°N and ~52°N, respectively), causing the January temperatures in NW Europe to be as low as −15°C to −25°C. During the two transitions these sea ice margins shifted to a location northwards of 60°N, allowing incursion of relatively warm ocean waters, in turn providing a heat source for Europe. This resulted in January temperatures that were 10°C to 25°C higher than during the stadial conditions. Our model results clearly illustrate that the position of the sea ice margin after the transition determines the pattern of the increase in January temperature. For instance, we prescribed ice-covered Nordic seas in expGI-1e, resulting in a maximum increase of January temperatures of 25°C centred at 57°N (see expGI-1e minus expGS-2a anomaly, Fig. 4f). In contrast, in expPB we assumed that the Nordic seas were free of sea ice, causing a maximum warming in northernmost Europe in the expPB minus expGS-1 anomaly (Fig. 8f).

This difference is also evident in the sea level pressure plots (Fig. 12b and d). In the expPB-result an extension of the Icelandic Low towards Scandinavia is visible, implying a regular inflow of relatively mild and moist oceanic air in this region, whereas in the expGI-1e plot the pressure is relatively high in this region, suggesting more cold and dry conditions in northernmost Europe.

We inferred that the increase in July temperature was mainly driven by two factors: (1) the summer insolation and (2) the ice sheets. The warming of the N Atlantic Ocean appears to have had a minor effect on the July temperature increase. From the present climate we know that the July temperature distribution in Europe depends primarily on the latitudinal distribution of solar radiation (causing a N–S temperature gradient). As discussed in Section 2.1, the summer insolation was relatively strong compared to today, with the anomaly increasing at 50°N from $+18$ W/m^2 during GS-2a to $+34$ W/m^2 during PB. Consequently, these high values forced the July temperatures to be relatively high during GS-2a (i.e. between 10°C and 20°C in NW Europe). As a result, the increase of July temperature during the transitions was small (generally less than 6°C) compared to the January conditions. The model results indicate that deglaciated regions formed an exception to this observation, as the July temperatures increased here by up to 10°C in the model. This shows that the proximity of the ice sheets had a strong tempering effect on the July temperatures.

On the basis of previously published model sensitivity studies it may be argued that the effect of other changed boundary conditions (i.e. concentration of greenhouse gases and vegetation parameters) on the 14.7 and 11.5 k transitions was relatively small. The consequence of the changed atmospheric concentrations of greenhouse gasses (i.e. CO_2, CH_4 and N_2O) is modest because the dominant part of their effect is incorporated in the prescribed SSTs and sea ice. This is clarified by, for instance, the work of Kutzbach and Guetter (1986), who found that a lowering of the atmospheric CO_2 concentration from 330 to 200 ppm in an AGCM simulation resulted in a cooling of only 0.2°C over Northern Hemisphere land surfaces. The effect of vegetation changes was studied in an earlier paper, in which it was concluded that it might have a relevant effect under specific circumstances (Renssen and Lautenschlager, 2000). Especially the percentage of land surface covered with trees appeared to be important, as this controls the surface albedo during winter. A sensitivity experiment suggested that a change from a tree-less landscape to a closed forest may cause a local temperature increase of 3°C. However, in the experiments discussed in the present paper, we assumed that the percentage of land surface covered with trees changed relatively little during the transitions. Going from GS-2a to GI-1e the landscape in NW Europe remained tree-less due to slow migration rates of trees and an absence of a favourable substrate (e.g. Paus, 1995; Hoek, 1997). Moreover, during GS-1 trees were more common in Europe, implying that the increase in forest density was not sufficient to evoke a large climatological effect.

4.3.5. Implications for registration of shifts in proxy data

The determination of the effect of different boundary conditions enables us to discuss expected implications for proxy data. Obviously, the position of various regions in Europe relative to changes in important boundary conditions (i.e. sea ice margin, ice sheets) during the two climate transitions varied. As a result, it is expected that the registration of the magnitude of the two transitions in terrestrial proxy records was geographically different. This implies that reconstructed temperature curves from various sites in Europe should show different magnitudes. Moreover, the timing of the two major shifts probably varied from place to place, as this timing is mainly determined by the position of the sea ice and land ice (c.f. Coope and Lemdahl, 1995). For instance, in N Norway the timing of the major warming is expected to be later than in Ireland, because in the North the ocean remained covered with sea ice and the Scandinavian ice sheet remained present until the early Holocene.

5. Conclusions

In this paper we characterised the major climate transitions in Europe during the last glacial–interglacial transition at 14.7 and 11.5 k by comparing maps of January and July temperatures obtained by two independent methods: (1) simulations with an atmospheric general circulation model and (2) reconstructions based on geological and palaeoecological data. In addition we compared estimates of lake level change with simulated P-E values. Based on these comparisons we conclude the following:

(1) The increase in January temperature during both 14.7 and 11.5 k transitions was up to 20°C in NW Europe, as January temperatures increased from −25°C to −15°C in GS-2a and GS-1 to values between −5°C and 5°C in GI-1e and PB.

(2) The July conditions during the two transitions changed less dramatically, as July temperatures increased in NW Europe by about 3–5°C from about 10°C to 15°C during GS-2a and GS-1 to 13°C to 17°C in GI-1e and PB. In S Europe the July warming appears to be less intense.

(3) Our comparison suggests that the effective precipitation remained at the same level during the 14.7 k transition. For the 11.5 k transition a small increase is found in some regions. The small net effect in effective precipitation (compared to temperature) is explained by similar increases in precipitation and evaporation during both transitions.

(4) The main factor driving the January temperature increase during both climate transitions was the N Atlantic Ocean. The change in SSTs and in the position of the sea ice margin determined the temperature change over land. The location of the sea ice margin before and after the transition controls the pattern of the January temperature increase. The model simulations indicate that this pattern appears to have been different for the two climatic shifts, with the major temperature increase being positioned near the Atlantic coast during the 14.7 k transition and in northernmost Europe during the 11.5 k transition.

(5) The increase in July temperatures was mainly determined by the increase in summer insolation but modified by the deglaciation in Scandinavia and Scotland. Compared to the changes in the Atlantic Ocean, the insolation changes were gradual (2 to 3 W/m^2 over the transitions), thus explaining the relatively small temperature increase in July compared to January. The climate model results suggested that July temperatures increased by up to 10°C in regions where land ice disappeared during the transitions.

(6) Our analyses suggest that the registration of the magnitude of the two climate transitions in terrestrial proxy records was geographically different due to the changing environmental conditions; shifts in the N Atlantic sea ice margin appear to be the most important. This implies that reconstructed temperature curves from different places in Europe should show different magnitudes. Moreover, it is to be expected that the timing of the major warming phases is spatially different, as this timing is controlled by the location of the sea ice and land ice margins relative to the place of interest.

Acknowledgements

We would like to thank J.-L. de Beaulieu for his information on botanical data from eastern France. We are indebted to the Max-Planck-Institute für Meteorologie (in particular L. Bengtsson) and the Deutsches Klimarechenzentrum (in particular M. Lautenschlager) for providing computing facilities for the modeling experiments. This manuscript benefitted greatly from the critical remarks of M. Kageyama, S. Björck, W. Hoek and J. Vandenberghe. The research was funded by the Dutch National Research Programme on Global Air Pollution and Climate Change (Contract number 951245).

Appendix A. References used in Table 3

Allen, J.R.M., Huntley, B., Watts, W.A., 1996. The vegetation and climate of northwest Iberia over the last 14,000 years. Journal of Quaternary Science 11, 125–147.

Ammann, B., 1989. Late-Quaternary palynology at Lobsigensee. Dissertationes Botanicae 137, 150.

Andrieu, V., Huang, C.C., O'Connell, M., Paus, A., 1993. Lateglacial vegetation in Ireland: first results from four western sites. Quaternary Science Reviews 12, 681–705.

Bałaga, K., 1990. The development of Lake Lukcze and changes in the plant cover of the south-western part of the Leczna–Wlodawa lake district in the last 13 000 years. Acta Palaeobotanica 30, 77–146.

Bartley, D.D., 1962. The stratigraphy and pollen analysis of lake deposits near Tadcaster, Yorkshire. New Phytologist 61, 277–287.

Bartley, D.D., Morgan, A.V., 1990. The palynological record of the King's Pool, Stafford, England. New Phytologist 116, 177–194.

Bartley, D.D., Chambers, C., Hart-Jones, B., 1976. The vegetational history of parts of south and east Durham. New Phytologist 77, 437–468.

Beales, P.W., 1980. The Late Devensian and Flandrian vegetational history of Crose Mere, Shropshire. New Phytologist 85, 133–161.

Beaulieu, J.-L.d., and Goeury, C., 1987. Zonation automatique appliquée a l'analyse pollinique: exemple de la Narse d'Ampoix (Puy de Dome, France). Bulletin de l'Association française pour l'etude du Quaternaire 1, 49–61.

Beaulieu, J.L. de, 1977. Contribution pollenanalytique- L'histoire Tardiglaciaire et Holocène de la végétation des Alpes méridionales françaises. Thesis, Univ. Aix-Marseille, France.

Beckett, S.C., 1981. Pollen diagrams from Holderness, North Humberside. Journal of Biogeography 8, 177–198.

Behre, K.E., 1966. Untersuchungen zur spätglazialen und frühpostglazialen Vegetationsgeschichte Ostfrieslands. Eiszeitalter und Gegenwart 17, 69–84.

Bennett, K.D., 1983. Devensian Late-glacial and flandrian vegetational history at Hockham Mere, Norfolk, England. New Phytologist 95, 457–487.

Berglund, B., 1966. Late-Quaternary vegetation in eastern Blekinge, southeastern Sweden; a pollen-analytical study. Opera Botanica, 12.

Berglund, B.E., Ralska-Jasiewiczowa, M., 1986. Pollen analysis and pollen diagrams. In "Handbook of Holocene Palaeoecology and Palaeohydrology", Berglund, B. (Ed.), Wiley, Chichester, pp. 455–484.

Bertsch, A., 1961. Untersuchungen zur spätglazialen Vegetationsgeschichte Südwestdeutschlands. Flora 151, 243–280.

Beug, H.-J., 1976. Die spätglaziale und frühpostglaziale Vegetationsgeschichte im Gebiet des ehemaligen Rosenheimer Sees (Oberbayern). Botanische Jahrbücher der Systematik 95, 373–400.

Bińka, K., Cieśla, A., Łącka, B., Madeyska, T., Marciniak, B., Szeroczyńska, K. and Więckowski, K., 1991. The development of Błedowo Lake (central Poland)—a palaeoecological study. Studia Geologica Polonica 100, 83.

Bjelm, L., 1976. Deglaciation of the Smalard Highland, with special reference to deglaciation, ice thickness and chronology. Lundqua theses 2, 1–78.

Björck, S., Håkansson, S., 1982. Radiocarbon dates from Late Weichselian lake sediments in south sweden as a basis for chronostratigraphic subdivision. Boreas 11, 141–150.

Bock, W., Menke, B., Strehl, E., Ziemus, H., 1985. Neue Funde des Weichselspätglazials in Schleswig–Holstein. Eiszeitalter und Gegenwart 35, 161–180.

Bohncke, S., Kasse, C., Vandenberghe, J., 1995. Climate induced environmental changes during the Vistulian Lateglacial at Zabinko. Quaestiones Geographicae 4, 43–64.

Bortenschlager, S., 1984. Die Vegetationsentwicklung im Spätglazial: das Moor beim Lanser See III, ein Typprofil für die Ostalpen. Festschrift Welten, Dissertationes Botanicae 72, 71–79.

Bos, J.A.A., 1998. Aspects of Lateglacial–Early Holocene vegetation development in western Europe. PhD thesis. Utrecht, LPP contributions Series No. 10. Febodruk, Enschede, 240.

Böse, M., Brande, A., Müller, M., Rowinsky, V., Anstreicher, J., 1995. Landscape development in the terminal area of the Brandenburg Stage south of Potsdam. Guide Excursion B20, 14th International Congress INQUA, Berlin, 1995, 30.

Brande, A., 1980. Pollenanalytische Untersuchungen im Spätglazial und frühen Postglazial Berlins. Verhandlungen des Botanischen Vereins der Provinz Brandenburg 115, 21–72.

Brown, A.P., 1977. Late-Devensian and Flandrian vegetational history of Bodmin Moor, Cornwall. Philosophical Transactions of the Royal Society of London B 276, 251–320.

Casparie, W.A., Van Zeist, W., 1960. A Late-glacial deposit near Waskemeer (Prov. of Friesland). Acta Botanica Neerlandica 9, 191–196.

Caspers, G., 1993. Vegetationsgeschichtliche Untersuchungen zur Flußauenentwicklung and der Mittelweser im Spätglazial und Holozän. Abhandlungen aus dem Westfälischen Museum für Naturkunde, Münster 55, 101.

Charman, D.J., 1994. Late-glacial and Holocene vegetation history of the Flow country, northern Scotland. New Phytologist 127, 155–168.

Chen, S.-H., 1988. Neue Untersuchungen über die spät-und postglaziale Vegetationsgeschichte im Gebiet zwischen Harz und Leine (BRD). Flora 181, 147–177.

Clerc, J., 1988. "Récherches pollenanalytiques sur la paléoécologie Tardiglaciaire et Holocène du Bas-Dauphiné", Université D'Aix-Marseille.

Cleveringa, P., De Gans, W., Kolstrup, E., Paris, F.P., 1977. Vegetational and climatic developments during the Late Glacial and the early Holocene and aeolian sedimentation as recorded in the Uteringsveen (Drente, The Netherlands). Geologie en Mijnbouw 56, 234–242.

Coope, G.R., Dickson, J.H., McCutcheon, J.A., Mitchell, G.F., 1979. The Lateglacial and early postglacial deposit at Drumurcher, Co. Monaghan. Proceedings of the Royal Irish Academy 79B, 63–85.

Craig, A.J., 1978. Pollen percentage and influx analyses in south-east Ireland: a contribution to the ecological history of the Late-glacial period. Journal of Ecology 66, 297–324.

Cwynar, L.C., Watts, W.A., 1989. Accelerator-mass spectrometer ages for late glacial events at Ballybetagh, Ireland. Quaternary Research 31, 377–380.

Day, P., 1995. Devensian Late-glacial and early Flandrian environmental history of the Vale of Pickering, Yorkshire, England. Journal of Quaternary Science 11, 9–24.

De Klerk, P., 1998. Late Glacial and Early Holocene vegetation history in northern Vorpommern: a preliminary review of available pollen diagrams. Projectbericht: DFG-Schwerpunktprogramm 'Entwicklung der Geo-Biosphäre in den letzten 15.000 Jahren', Greifswald, 34.

Digerfeldt, G., 1982. The Holocene development of Lake Sambosjon.1. The regional vegetation history. Lundqua Report 23, 1–24.

Fredskild, B., 1975. A Late-glacial and early post-glacial pollen-concentration diagram from Langeland, Denmark. Geologiska Föreningens i Stockholm Förhandlingar 97, 151–161.

Fritz, A., 1965. Pollenanalytische Untersuchung zur spät- und postglazialen Vegetationsgeschichte im oberen Drautal, Kärnten. Carinthia II 75, 89–115.

Goslar, T., Bałaga, K., Arnold, M., Tisnerat, N., Starnawska, E., Kuzniarski, M., Chrost, L., Walanus, A., Wieckowski, K., 1999. Climate-related variations in the composition of the Lateglacial and Early Holocene sediments of Lake Perespilno (eastern Poland). Quaternary Science Reviews 18, 899–911.

Guenet, P., 1993. Analyses pollenanalytiques en Artense et sur le plateau de Millevanches (Massif Central, France). Palynosciences 2, 79–107.

Hahne, J., 1991. Untersuchungen zur spät-und postglazialen Vegetationsgeschichte im nördlichen Bayern (Rhön, Grabfeld, Lange Berge). Flora 185, 17–32.

Hahne, J., 1992. Untersuchungen zur spät-und postglazialen Vegetationsgeschichte im nordöstlichten Bayern (Bayrisches Vogtland, Fichtelgebirge, Steinwald). Flora 187, 169–200.

Hannon, G.E., 1985. Late Quaternary vegetation of Sanabria Marsh, North West Spain. Thesis. Trinity College, Dublin, Ireland.

Heider, S., 1995. Die Siedlungs-und Vegetationsgeschichte im Ostteil des Elbe-Weser-Dreiecks nach pollenanalytischen Untersuchungen. Probleme der Küstenforschung im südlichen Nordseegebiet 23, 51–115.

Heinz, C., Thiébault, S., 1998. Characterization and palaeoecological significance of archaeological charcoal assemblages during Late and post-glacial phases in southern France. Quaternary Research 50, 56–68.

Hoek, W.Z., Bohncke, S.J.P., Ganssen, G.M., Meijer, T., 1999. Lateglacial environmental changes recorded in calcareous gyttja deposits at Gulickshof, southern Netherlands. Boreas 28, 416–432.

Huntley, B., 1994. Late Devensian and Holocene palaeoecology and palaeoenvironments of the Morrone Birkwoods, Aberdeenshire, Scotland. Journal of Quaternary Science 9, 311–336.

Huttunen, A., Huttunen, R.-L., Vasari, Y., Panovska, H., Bozilova, E., 1992. Late-glacial and Holocene history of flora and vegetation in the Western Rhodopes Mountains, Bulgaria. Acta Botanica Fennica 144, 63–80.

Hyvarinen, H., 1985. Holocene pollen history of the Alta area, an isolated pine forest north of the general pine forest region in Fennoscandia. Ecolo. Medit. 11 (1), 69–71.

Iversen, J., 1954. The Late-glacial flora of Denmark and its relation to climate and soil. Danmarks Geologiske Undersøgelse 80, 87–119.

Jalut, G., 1967. Analyse pollinique de la tourbière de l'Archet. Pollen et Spores 9, 305–319.

Jalut, G., Delibrias, G., Dagnac, J., Mardiones, M., Bouhours, M., 1982. A palaeoecological approach to the last 21000 years in the Pyrenees: the peat bog of Freychinede (alt. 1350 m, AriSge, South France). Palaeogeography, Palaeoclimatology, Palaeoecology 40, 321–359.

Jalut, G., Monserrat Marti, J., Fontugne, M., Delibrias, G., Vilaplana, J.M., Julia, R., 1992. Glacial to interglacial vegetation changes in the northern and southern Pyrénées: degalciation, vegetation and chronology. Quaternary Science Reviews 11, 449–480.

Jankovska, V., 1980. Paläogeobotanische Rekonstruktion der Vegetationsentwicklung im Becken Trebonska panev während des Spätglazials und Holozäns. Vegetace CSSR, A11, 151.

Janssen, C.R., IJzermans-Lutgerhorst, W., 1973. A 'local' Lateglacial pollen diagram from Limburg, Netherlands. Acta Botanica Neerlandica 22, 213–220.

Járai-Komlódi, M., 1968. The Late glacial and Holocene flora of the Hungarian Great Plain. Annales Universitatis Scientarum Budapestinensis de Rolanda Eötvös Nominatae. Separatum Sectio Biologica 9–10, 199–225.

Jones, R.L., 1976. Late Quaternary vegetational history of the North York Moors. IV. Seamer Carrs. Journal of Biogeography 3, 397–406.

Knipping, M., 1989. Zur spät-und postglazialen Vegetationsgeschichte des Oberpfälzer Waldes. Dissertationes Botanicae 140, 209.

Kolstrup, E., Buchardt, B., 1982. A pollen analytical investigation supported by an ^{18}O-record of a late glacial lake deposit at Graenge (Denmark). Review of Palaeobotany and Palynology 36, 205–230.

Koperowa, W., 1961. The history of the Late-glacial and Holocene of the vegetation of the Nowy Targ basin (in Polish). Acta Palaeobotanica 1, 1–?.

Koperowa, W., 1962. The vegetation of the basin of Sandomierz in the Late-glacial and Holocene (in Polish). Acta Palaeobotanica 3, 1–66.

Lange, E., Jeschke, L., Knapp, H.-D., 1986. Ralswiek und Rügen. Landschaftsentwicklung und Siedlungsgeschichte der Ostseeinsel. (Berliner) Schriften zur Ur-und Frühgeschichte. Akademie Verlag Berlin 38, 175.

Liedberg-Jönsson, B., 1988. The Late Weichselian macrofossil flora in western Skåne, southern Sweden. Lundqua Thesis 24, 1–42.

Litt, T., 1988. Untersuchungen zur spätglazialen Vegetationsentwicklung bei Dziekanowice (Umgebung Lednogóra, Wielkopolska). Acta Palaeobotanica 28, 49–60.

Litt, T., 1994. Paläoökologie, Paläobotanik und stratigraphie des Jungquartärs im nordmitteleuropäischen Tiefland. Dissertationes Botanicae 227, 185.

Lotter, A., 1988. Paläoökologische und paläolimnologische Studie des Rotsees bei Luzern. Dissertationes Botanicae 124, 187.

Lowe, J.J., Walker, M.J.C., 1977. The reconstruction of the Lateglacial environment in the southern and eastern Grampian Highlands. In "Studies in the Scottish Lateglacial Environment", Gray, J.M., J.J. Lowe (Eds.), Pergamon, Oxford, pp. 101–118.

Magny, M., Schoellammer, P., Richard, H., Bossuet, G., 1998. A high-resolution record of Late Younger Dryas to Mid-Holocene palaeohydrological changes from the palaeolake Le Locle, Swiss Jura. Comptes Rendus de l'Académie de Sciences de Paris. Earth and Planetary Sciences 326, 787–793.

Marambat, L., Roussot-Larrogue, J., 1989. Paysage végétal et occupations humaines sur la cote Atlantique: l'exemple de la Lède du Gurp. Bulletin de LAFEQ 2, 73–89.

Mecke, A., 1995. Pollenanalytische Untersuchungen zur spät-und postglazialen Vegetations-und Klimageschichte im Landkreis Friesland. Probleme der Küstenforschung im südlichen Nordseegebiet 23, 11–49.

Menke, B., 1968. Das Spätglazial von Glüsing. Eiszeitalter und Gegenwart 19, 73–84.

Miotk-Szpiganowicz, G., 1992. The history of the vegetation of Bory Tucholski and the role of man in the light of palynological investigations. Acta Palaeobotanica 32, 39–122.

Mitchell, G.F., 1940. Studies in Irish Quaternary Deposits, some Lacustrine Deposits near Dunshaughlin, Co. Meath. Proc.R. Ir. Acad. 46-B, 13–37.

Moar, N.T., 1969b. Late Weichselian and Flandrian pollen diagrams from south-west Scotland. New Phytologist 68, 433–467.

Moar, N.T., 1969a. Two pollen diagrams from the Mainland, Orkney Islands. New Phytologist 68, 201–208.

Moore, P.D., 1970. Studies in the vegetational history of mid-Wales. II. The Late-glacial period in Cardiganshire. New Phytologist 69, 363–375.

Müller, H., 1953. Zur spät-und nacheiszeitlichen Vegetationsgeschichte des mitteldeutschen Trockengebietes. Nova Acta Leopoldina 110, 67.

Munaut, A.V., Paulissen, E., 1973. Evolution et paléo-ecologie de la Vallée de la Petite Nèthe au cours du Post-Würm (Belgique). Annales de la Société Géologique de Belgique 96, 310–348.

Noryśkiewicz, B., 1982. Lake Steklin—A reference site for the Dobrzyń-Chełmno Lake District, N. Poland. Report on Palaeoecological Studies for the IGCP-Project No. 158 B. Acta Palaeobotanica 22, 65–83.

O'Connell, M., Huang, C.C., Eicher, U., 1999. Multidisciplinary investigations, including stable-isotope studies, of thick Late-glacial sediments from Torry Hill, Limerick, western Ireland. Palaeogeography, Palaeoclimatology, Palaeoecology 147, 169–208.

Oldfield, F., 1964. Late-Quaternary deposits at Le Moura, Biarritz, south-west France. New Phytologist 63, 374–409.

Paus, A., 1988. Late Weichselian vegetation, climate, floral migration at Sandvikvatn, North Rogaland, southwestern Norway. Boreas 17, 113–139.

Paus, A., 1989. Late Weichselian vegetation, climate and floral migration at Liastemmen, North Rogaland, south-western Norway. Journal of Quaternary Science 4, 223–242.

Pawlikowski, M., Ralska-Jasiewiczowa, M., Schönborn, W., Stupnicka, E., Szeroczynska, K., 1982. Woryty near Gietrzwald, Olsztyn Lake District, NE Poland—vegetational history and lake development during the last 12000 years. Acta Palaeobotanica 22, 85–116.

Peglar, S., 1979. A radio-carbon dated pollen diagram from Loch Winless, Caithness, north-east Scotland. New Phytologist 82, 245–263.

Penalba, M.C., 1994. The history of the Holocene vegetation in northern Spain from pollen analysis. Journal of Ecology 82, 815–832.

Penalba, M.C., Arnold, M., Guiot, J., Duplessy, J.-C., De Beaulieu, J.-L., 1997. Termination of the Last Glaciation in the Iberian Peninsula inferred from the pollen sequence of Quintanar de la Sierra. Quaternary Research 48, 205–214.

Pérez-Obiol, R., Julia, R., 1994. Climatic change on the Iberian Peninsula recorded in a 30,000-yr pollen record from Lake Banyoles. Quaternary Research 41, 91–98.

Philisophical Transactions of the Royal Society of London Series B 318, 451–485.

Pilcher, J.R., Larmour, R., 1982. Late-glacial and post-glacial vegetational history of the Meenadoan nature reserve, County Tyrone. Proceedings of the Royal Irish Academy 82B 277–295.

Pons, A., Reille, M., 1988. The Holocene and upper Pleistocene pollen record from Padul (Granada, Spain): a new study. Palaeogeography, Palaeoclimatology, Palaeoecology 66, 243–263.

Ralska-Jasiewiczowa, M., 1966. Bottom sediments of the Mikolajki lake (Masurian Lake District) in the light of palaeobotanic investigations. Acta Palaeobotanica 7, 1–118.

Ralska-Jasiewiczowa, M., 1980. Late-glacial and Holocene vegetation of the Bieszczady Mts. (polish eastern Carpathians). Polska Akademia Nauk, 196.

Ralska-Jasiewiczowa, M., Van Geel, B., Goslar, T., Kuc, T., 1992. The record of the Late Glacial/Holocene transition in the varved sediments of Lake Gosciaz, central Poland. Sveriges Geologiska Undersökning 81, 257–268.

Rehagen, H.-W., 1064. Zur spät-und postglazialen Vegetationsgeschichte des Niederrheingebietes und Westmünsterlandes. Fortschritte der Geologie in Rheinland und Westfalen 12, 55–96.

Reille, M., 1993. L'interface Tardiglaciaire-Holocène dans un site du littoral atlantique sud-européen: Le Moura (Pyrénées Atlantiques, France). C.R. Acad. Sci. Paris, Sciences de la vie 316, 463–468.

Reille, M., Lowe, J.J., 1993. A re-evaluation of the vegetation history of the eastern Pyrenees (France) from the end of the last glacial to the present. Quaternary Science Reviews 12, 47–77.

Rösch, M., 1985. Nussbaumer Seen- spät-und postglaziale Umweltveränderungen einer Seengruppe im östlichen Schweizer Mittelland. Dissertationes Botanicae 87, 337–379.

Rybníçková, E., 1974. Die Entwicklung der Vegetation und Flora im südlichen Teil der Böhmisch-Märischen Höhe während des Spätglazials und Holozäns. Vegetace CSSR A7, 163.

Rymer, L., 1977. A Late-glacial and early Postglacial pollen diagram from Drimnagall, north Knapdale, Argyllshire. New Phytologist 79, 211–221.

Schloss, S., 1979. Pollenanalytische und stratigraphische Untersuchungen im Sewensee; ein Beitrag zur spätglazialen Vegetationsgeschichte der Südvogesen. Dissertationes Botanicae 52, 119.

Smith, A.G., Goddard, I.C., 1991. A 12.5000 year record of vegetational history at Sluggan Bog, Co. Antrim, N. Ireland (incorporating a pollen zone for the non-specialist). New Phytologist 118, 167–187.

Stalling, H., 1987. Untersuchungen zur spät-und postglazialen Vegetationsgeschichte im Bayerischen Wald. Dissertation Göttingen, 153.

Stockmarr, J., 1974. Biostratigraphic studies in Late Weichselian sediments near Böllingsö. Danmarks geoligiska Undersögelske, Arbog 1974, 71–89.

Streitz, B., 1980. Vegetationsgeschichtliche und pflanzensoziologische Untersuchungen an zwei Mooren Osthessischer Subrosionssenken. Dissertation Darmstadt, 158.

Svensson, N.-O., 1989. Late Weichselian and early Holocene

shore displacement in the central Baltic, based on stratigraphical and morphological records from eastern Smäland and Gotland. Lundqua Thesis 25, 195.

Szczepanek, K., 1982. Development of the peat-bog at Słopiec and the vegetational history of the Świętokrzyskie (Holy Cross) Mts. in the last 10000 years. Acta Palaeobotanica 22, 117–130.

Turner, C., Hannon, G.E., 1988. Vegetational evidence for late Quaternary climate changes in southwest Europe in relation to the influence of the North Atlantic Ocean.

Usinger, H., 1977. Bölling-Interstadial und Laacher Bimstuff in einem neuen Spätglazial-Profil aus dem Vallensgård Mose/Bornholm. Mit pollengrößenstatistischer Trennung der Birken. Danmarks Geologiske Undersøgelse, Årbog 1977, 5–29.

Usinger, H., 1981b. Zur spät-und postglazialen Vegetationsgeschichte der Schleswig–Holsteinischen Geest nach einem Pollen-und Pollendichtediagramm aus dem Esinger Moor. Pollen et Spores 23, 389–427.

Usingear, H., 1982. Pollenanalytische Untersuchungen an spätglazialen und präborealen Sedimenten aus dem Meerfelder Maar (Eifel). Flora 172, 373–409.

Usinger, H., Wolf, A., 1982. Zur vegetations-und klimageschichtliche Gliederung des Alleröds nach Untersuchungen im Blixmoor und Kubitzbergmoor (Schleswig–Holstein). Schrifte des Naturwissenschaftlichen Vereins von Schleswig–Holstein 52, 29–45.

Van der Knaap, W.P., Van Leeuwen, J.F.N., 1997. Late Glacial and early Holocene vegetation succession, altitudinal vegetation zonation, and climatic change in the Serra da Estrella, Portugal. Review of Palaeobotany and Palynology 97, 239–285.

Van Geel, B., Coope, G.R., Van der Hammen, T., 1989. Palaeoecology and stratigraphy of the lateglacial type section at Usselo (the Netherlands). Review of Palaeobotany and Palynology 60, 25–129.

Van Zeist, W., Van der Spoel-Walvius, M.R., 1980. A palynological study of the Late-Glacial and the Postglacial in the Paris Basin. Palaeohistoria 22, 67–109.

Verbruggen, C.L.H., 1979. Vegetational and palaeoecological history of the Lateglacial period in Sandy Flanders (Belgium). Acta Universitatis Ouluensis A 82, 133–142.

Walker, M.J.C., Harkness, D.D., 1990. Radiocarbon dating the Devensian Lateglacial in Britain: new evidence from Llanilid, South Wales. Journal of Quaternary Science 5, 134–144.

Walker, M.J.C., 1982. The Late-glacial and early Flandrian deposits at Traeth Mawr, Brecon Beacons, South Wales. New Phytologist 90, 177–194.

Watts, W.A., 1963. Late-Glacial polen zones in western Ireland. Irish Geog. 4, 367–376.

Watts, W.A., Allen, J.R.M., Huntley, B., Fritz, S.C., 1996. Vegetation history and climate of the last 15,000 years at Laghi di Montecchio, southern Italy. Quaternary Science Reviews 15, 113–132.

Watts, W.A., 1977. The Late Devensian vegetation of Ireland. Philosophical Transactions of the Royal Society of London B 280, 273–293.

Webb, J.A. and Moore, P.D., 1982. The Late Devensian vegetational history of the Whitlaw Mosses, southeast Scotland. New Phytologist 91, 341–398.

Wegmüller, S., 1977. Pollenanalytische Untersuchungen zur spät-und postglazialen Vegetationsgeschichte der französischen Alpen (Dauphin). Verlag Paul Haupt, Bern, 185.

Wegmüller, S., 1997/8. Vegetations-und siedlungsgeschichtliche Untersuchungen an einem Bohrprofil von Langnau i.E. Mitteilungen der Naturforschenden Gesellschaft in Bern 103–134.

Wegmüller, S., Lotter, A.F., 1990. Palynostratigraphische Untersuchungen zur spät-und postglazialen Vegetationsgeschichte der nordwestlichen Kalkalpen. Botanicae Helvetica 100, 37–73.

Woillard, G., 1975. Récherches palynologiques sur le Pléistocène dans l'Est de la Belgique et dans les Vosges Lorraines. Acta Geographica Lovaniensia 14, 118.

Zachowicz, J., Przybylowska-Lange, W., Nagler, J., 1982. The Late-glacial and Holocene vegetational history of the Zulawy region, N. Poland. A biostratigraphic study of lake sediments. Acta Palaeobotanica 22, 141–161.

References

Adams, J.M., 1997. Europe during the last 150,000 years. Environmental Sciences Division, Oak Ridge National Laboratory, USA, at http://www.esd.ornl.gov.

Alley, R.B., Meese, D.A., Shuman, C.A., Gow, A.J., Taylor, K.C., Grootes, P.M., White, J.W.C., Ram, M., Waddington, E.D., Mayewski, P.A., Zielinski, G.A., 1993. Abrupt increase in Greenland snow accumulation at the end of the Younger Dryas event. Nature 362, 527–529.

Ammann, B., 1989. Late-Quaternary palynology at Lobsigensee. Dissertationes, 137.

Andrieu, V., Huang, C.C., O'Connell, M., Paus, A., 1993. Lateglacial vegetation in Ireland: first results from four western sites. Quaternary Science Reviews 12, 681–705.

Atkinson, T.C., Briffa, K.R., Coope, G.R., 1987. Seasonal temperatures in Britain during the past 22,000 years, reconstructed using beetle remains. Nature 325, 587–591.

Bałaga, K., 1990. The development of Lake Lukcze and changes in the plant cover of the south-western part of the Leczna–Włodowa Lake district in the last 13000 years. Acta Palaeobotanica 30, 77–146.

Ballantyne, C.K., Harris, C., 1994. The Periglaciation of Great Britain. Cambridge Univ. Press, Cambridge, 330 pp.

Barnola, J.M., Raynaud, D., Korotkevich, Y.S., Lorius, C., 1987. Vostok ice core provides 160000-year record of atmospheric CO_2. Nature 329, 408–414.

Bateman, M.D., Van Huissteden, J., 1999. The timing of last-glacial periglacial and aeolian events, Twente, eastern Netherlands. Journal of Quaternary Science 14, 277–283.

Berger, A.L., 1978. Long-term variations of caloric insolation resulting from the earth's orbital elements. Quaternary Research 9, 139–167.

Beug, H.-J., 1976. Die spätglaziale und frühpostglaziale Vegetationsgeschichte im Gebiet des ehemaligen Rosenheimer Sees

(Oberbayern). Botanische Jahrbücher der Systematik 95, 373–400.
Bjelm, L., 1976. Deglaciation of the Smalard Highland, with special reference to deglaciation, ice thickness and chronology. Lundqua Theses 2, 1–78.
Björck, S., Walker, M.J.C., Cwynar, L.C., Johnsen, S., Knudsen, K.-L., Lowe, J.J., Wohlfarth, B., INTIMATE Members, 1998. An event stratigraphy for the Last Termination in the North Atlantic region based on the Greenland ice-core record: a proposal by the INTIMATE group. Journal of Quaternary Science 13, 283–292.
Bond, G., Broecker, W., Johnsen, S., McManus, J., Labeyrie, L., Jouzel, J., Bonani, G., 1993. Correlations between climate records from North Atlantic sediments and Greenland ice. Nature 365, 143–147.
Bos, J.A.A., 1998. Aspects of Lateglacial–Early Holocene vegetation development in western Europe. PhD thesis, Utrecht, LPP contributions Series No. 10. Febodruk, Enschede, 240 pp.
Burn, C.R., 1990. Implications for palaeoenvironmental reconstructions of recent ice-wedge development at Mayo, Yukon Territory. Permafrost and Periglacial Processes 1, 3–14.
Claussen, M., Lohmann, U., Roeckner, E., Schulzweida, U., 1994. A global data set of land-surface parameters. Max-Planck-Institut für Meteorologie report no. 135, Hamburg, 30 pp.
Clerc, J., 1988. Récherches pollenanalytiques sur la paléoécologie Tardiglaciaire et Holocène du Bas-Dauphiné, Thesis Université D'Aix-Marseille, 179 pp.
CLIMAP members, 1981. Seasonal reconstructions of the earth's surface at the Last Glacial Maximum. Geological Society of America, Map and Chart Series MC-36.
COHMAP members, 1988. Climatic changes of the last 18,000 years: observations and model simulations. Science 241, 1043–1052.
Coope, G.R., Lemdahl, G., 1995. Regional differences in the Lateglacial climate of northern Europe based on coleopteran analysis. Journal of Quaternary Science 10, 391–395.
Coope, G.R., Lemdahl, G., Lowe, J.J., Walkling, A., 1998. Temperature gradients in Northern Europe during the Last Glacial–Interglacial Transition (14-9 14C ka BP) interpreted from Coleopteran Assemblages. Journal of Quaternary Science 13, 419–433.
Crowley, T.J., 1994. Pleistocene temperature changes. Nature 371, 664.
de Vernal, A., Hillaire-Marcel, C., Turon, J.L., Matthiessen, J., 2000. Reconstruction of sea-surface temperature, salinity, and sea-ice cover in the northern North Atlantic during the last glacial maximum based on dinocyst assemblages. Canadian Journal of Earth Sciences 37, 725–750.
DKRZ, 1994. The ECHAM 3 Atmospheric General Circulation Model. Deutsches Klimarechenzentrum, Technical Report no. 6, 184 pp.
Dwucet, K., Sniesko, Z., 1996. Neopleistocene loess cover evolution: an example from the Odonow sedimentary succession (southern Poland). Biuletyn Peryglacjalny 35, 7–30.
Fassl, K., 1996. Die Bewertung von Zeigerarten in europäischen Pollendiagrammen für die Rekonstruktiondes Klimas im Holozän. Palaeoklimaforschung, vol. 22, Gustav Fischer Verlag, Stuttgart-Jena-New York, p. 371.
Fawcett, P.J., Ágústsdóttir, A.M., Alley, R.B., Shuman, C.A., 1997. The Younger Dryas termination and North Atlantic Deep Water formation: insight from climate model simulations and Greenland ice cores. Paleoceanography 12, 23–38.
Felzer, B., Webb III, T., Oglesby, R.J., 1998. The impact of ice sheets, CO_2, and orbital insolation on Late Quaternary climates: sensitivity experiments with a general circulation model. Quaternary Science Reviews 17, 507–534.
Goździk, J.S., 1986. Structures de fentes a remplissage primaire sableux du Vistulien en Pologne et leur importance paléogéographique. Biuletyn Peryglacjalny 31, 71–105.
Goździk, J.S., 1995. Permafrost evolution and its impact on deposition conditions between 20 and 10 ka BP in Poland. Biuletyn Peryglacjalny 34, 53–72.
Greig, D.C., 1981. Ice-wedge cast network in eastern Berwickshire. Scottish Journal of Geology 17, 119–122.
Guilderson, T.P., Fairbanks, R.G., Rubenstone, J.L., 1994. Tropical temperature variations since 20,000 years ago: modulating interhemispheric climate change. Science 263, 663–665.
Habbe, K.A., 1993. Permafrost in glaciofluvial sediments of the Late Pleniglacial of the last Glaciation- and some conclusions to draw. Zeitschrift für Geomorphologie N.F. 92, 97–111.
Hahne, J., 1991. Untersuchungen zur spät-und postglazialen Vegetationsgeschichte im nördlichen Bayern (Rhön, Grabfeld, Lange Berge). Flora 185, 17–32.
Harrison, S.P., Digerfeldt, G., 1993. European lakes as palaeohydrological and palaeoclimatic indicators. Quaternary Science Reviews 12, 233–248.
Heinz, C., Thiébault, S., 1998. Characterization and palaeoecological significance of archaeological charcoal assemblages during Late and post-glacial phases in southern France. Quaternary Research 50, 56–68.
Helluin, M., Lautridou, J.-P., Ozouf, J.-C., 1977. Loess et fentes de gel de la Briqueterie de Glos pres de Lisieux (Calvados). Bulletin de la Societe. Linneenne de Normandie 105, 45–56.
Hoek, W.Z., 1997. Palaeogeography of Lateglacial Vegetations. Aspects of Lateglacial and Early Holocene vegetation, abiotic landscape, and climate in The Netherlands. Netherlands Geographical Studies 230, 146.
Huijzer, A.S., Isarin, R.F.B., 1997. The reconstruction of past climates using multi-proxy evidence; an example of the Weichselian Pleniglacial in northwest and central Europe. Quaternary Science Reviews 16, 513–533.
Huijzer, B., Vandenberghe, J., 1998. Climatic reconstruction of the Weichselian Pleniglacial in northwestern and central Europe. Journal of Quaternary Science 13, 391–417.
Huisink, M., 2000. Changing river styles in response to Weichselian climate changes in the Vecht valley, eastern Netherlands. Sedimentary Geology 133, 115–134.
Huttunen, A., Huttunen, R.-L., Vasari, Y., Panovska, H., Bozilova, E., 1992. Late-glacial and Holocene history of flora and vegetation in the Western Rhodopes Mountains, Bulgaria. Acta Botanica Fennica 144, 63–80.
Isarin, R.F.B., 1997. Permafrost distribution and temperatures in Europe during the Younger Dryas. Permafrost and Periglacial Processes 8, 313–333.
Isarin, R.F.B., Bohncke, S.J.P., 1999. Mean July temperatures during the Younger Dryas in northwestern and central Europe

as inferred from climate indicator species. Quaternary Research 51, 158–173.

Isarin, R.F.B., Renssen, H., 1999. Reconstructing and modelling Late Weichselian climates: the Younger Dryas in Europe as a case study. Earth-Science Reviews 48, 1–38.

Isarin, R.F.B., Renssen, H., Koster, E.A., 1997. Surface wind climate during the Younger Dryas in Europe as inferred from aeolian records and model simulations. Palaeogeography, Palaeoclimatology, Palaeoecology 134, 127–148.

Isarin, R.F.B., Renssen, H., Vandenberghe, J., 1998. The impact of the North Atlantic ocean on the Younger Dryas climate in north-western and central Europe. Journal of Quaternary Science 13, 447–453.

Iversen, J., 1954. The Late-glacial flora of Denmark and its relation to climate and soil. Danmarks geologiske Undersögelse II 80, 87–119.

Jalut, G., Monserrat Marti, J., Fontugne, M., Delibrias, G., Vilaplana, J.M., Julia, R., 1992. Glacial to interglacial vegetation changes in the northern and southern Pyrénées: degalciation, vegetation and chronology. Quaternary Science Reviews 11, 449–480.

John, B.S., 1973. Vistulian periglacial phenomena in south-west Wales. Biuletyn Peryglacjalny 22, 185–213.

Kageyama, M., Valdes, P.J., 2000. Impact of the North American ice-sheet orography on the Last Glacial Maximum eddies and snowfall. Geophysical Reserach Letters 27, 1515–1518.

Kageyama, M., Valdes, P.J., Ramstein, G., Hewitt, C., Wyputta, U., 1999. Northern Hemisphere storm tracks in present day and last glacial maximum climate simulations: a comparison of the European PMIP models. Journal of Climate 12, 742–760.

Koç, N., Jansen, E., Haflidason, H., 1993. Paleoceanographic reconstructions of surface ocean conditions in the Greenland, Iceland and Norwegian Seas through the last 14 ka based on diatoms. Quaternary Science Reviews 12, 115–140.

Koç, N., Jansen, E., Hald, M., Labeyrie, L., 1996. Late-glacial–Holocene sea surface temperatures and gradients between the North Atlantic and the Norwegian Sea: implications for the Nordic heat pump. In: Andrews, J.T., Austin, W.E.N., Bergsten, H., Jennings, A.E. (Eds.), Late Quarternary Palaeoceanography of the North Atlantic Margins. Geological Society Special Publication, London, pp. 177–185.

Kohfeld, K.E., Harrison, S.P., 2000. How well can we simulate past climates? Evaluating the models using global palaenvironmental datasets. Quaternary Science Reviews 9, 321–346.

Kolstrup, E., 1980. Climate and stratigraphy in Northwestern Europe between 30,000 BP and 13,000 BP with special reference to the Netherlands. Mededelingen Rijks Geologische Dienst 32, 253 pp.

Kolstrup, E., Mejdahl, V., 1986. Three frost wedge casts from Jutland (Denmark) and TL dating of their infill. Boreas 15, 311–321.

Koperowa, W., 1962. The vegetation of the basin of Sandomierz in the Late-glacial and Holocene (in Polish). Acta Palaeobotanica 3, 1–66.

Kozarski, S., 1993. Late Plenivistulian deglaciation and the expansion of the periglacial zone in NW Poland. Geologie en Mijnbouw 72, 143–157.

Kutzbach, J.E., Guetter, P.J., 1986. The influence of changing orbital parameters and surface boundary conditions on climate simulations for the past 18 000 years. Journal of the Atmospheric Sciences 43, 1726–1759.

Kutzbach, J.E., Guetter, P.J., Behling, P.J., Selin, R., 1993. Simulated climatic changes: results of the COHMAP climate-model experiments. In: Wright Jr., H.E., Kutzbach, J.E., Webb III, T., Ruddiman, W.F., Street-Perrott, F.A., Bartlein, P.J. (Eds.), Global climates since the Last Glacial Maximum. University of Minnesota Press, Minneapolis, pp. 24–93.

Kutzbach, J.E., Gallimore, R., Harrison, S., Behling, P., Selin, R., Laarif, F., 1998. Climate and biome simulations for the past 21,000 years. Quaternary Science Reviews 17, 473–506.

Lautridou, J.-P., 1985. Le cycle périglaciaire Pléistocène en Europe du Nord-Ouest. Thesis University of Caen, France, 908 pp.

Lewis, C.A., 1977. Ice-wedge casts in north-east County Wicklow. Scientific Proceedings, Royal Dublin Society 6A, 17–35.

Liedtke, H., 1957–1958. Frostbodenstrukturen aus dem norddeutschen Jungmoränengebiet. Wissenschaftliche Zeitschrift der Humboldt-Universität zu Berlin Mathematische/Naturwissenschaftliche Reihe 3, 359–376.

Lowe, J.J., Coope, G.R., Lemdahl, G., Walker, M.J.C., 1995. The Younger Dryas climate signal in land records from NW Europe. In: Troelstra, S.R., van Hinte, J.E., Ganssen, G.M. (Eds.), The Younger Dryas. Proceedings of a Workshop at the Royal Netherlands Academy of Arts and Sciences on 11–13 April 1994, Amsterdam, pp. 3–25.

Lowe, J.J., Birks, H.H., Brooks, S.J., Coope, G.R., Harkness, D.D., Mayle, F.E., Sheldrick, C., Turney, C.S.M., Walker, M.J.C., 1999. The chronology of palaeoenvironmental changes during the Last Glacial–Holocene transition: towards an event stratigraphy for the British Isles. Journal of the Geological Society of London 156, 397–410.

Magny, M., Ruffaldi, P., 1995. Younger Dryas and early Holocene lake-level fluctuations in the Jura mountains, France. Boreas 24, 155–172.

Manabe, S., Stouffer, R.J., 1997. Coupled ocean–atmosphere model response to freshwater input: comparison to Younger Dryas event. Paleoceanography 12, 321–336.

Mikolajewicz, U., Crowley, T.J., Schiller, A., Voss, R., 1997. Modelling teleconnections between the North Atlantic and North Pacific during the Younger Dryas. Nature 387, 384–387.

Olson, J.S., Watts, J.A., Allison, L.J., 1983. Carbon in Live Vegetation of Major World Ecosystems, ORNL-5862, ESD Pub No. 1997, Oak Ridge National Laboratory, Oak Ridge, Tennessee.

Paus, A., 1995. The Late Weichselian and early Holocene history of tree birch in south Norway and the Bölling Betula time-lag in northwest Europe. Review of Palaeobotany and Palynology 85, 243–262.

Peltier, W.R., 1994. Ice age paleotopography. Science 265, 195–201.

Pérez-Obiol, R., Julia, R., 1994. Climatic change on the Iberian Peninsula recorded in a 30,000-yr pollen record from Lake Banyoles. Quaternary Research 41, 91–98.

Péwé, T.L., 1966. Paleoclimatic significance of fossil ice wedges. Biuletyn Periglacjalny 15, 65–73.

Pinot, S., Ramstein, G., Harrison, S.P., Prentice, I.C., Guiot, J., Stute, M., Joussaume, S., PMIP participating groups, 2000. Tropical paleoclimates at the Last Glacial Maximum: comparison of Paleoclimate Modeling Intercomparison Project (PMIP) simulations and paleodata. Climate Dynamics 15, 857–874.

Pons, A., Reille, M., 1988. The Holocene and upper Pleistocene pollen record from Padul (Granada, Spain): a new study. Palaeogeography, Palaeoclimatology, Palaeoecology 66, 243–263.

Rasmussen, T.L., Thomsen, E., Labeyrie, L., van Weering, T.C.E., 1996a. Circulation changes in the Faeroe-Shetland Channel correlating with cold events during the last glacial period (58–10 ka). Geology 24, 937–940.

Rasmussen, T.L., Thomsen, E., van Weering, T.C.E., Labeyrie, L., 1996b. Rapid changes in surface and deep water conditions at the Faeroe margin during the last 58,000 years. Paleoceanography 11, 757–771.

Raynaud, D., Jouzel, J., Barnola, J.M., Chappellaz, J., Delmas, R.J., Lorius, C., 1993. The ice record of greenhouse gases. Science 259, 926–933.

Renssen, H., 1997. The global response to Younger Dryas boundary conditions in an AGCM simulation. Climate Dynamics 13, 587–599.

Renssen, H., Isarin, R.F.B., 1998. Surface temperature in NW Europe during the Younger Dryas: AGCM simulation compared with temperature reconstructions. Climate Dynamics 14, 33–44.

Renssen, H., Lautenschlager, M., 2000. The effect of vegetation in a climate model simulation on the Younger Dryas. Global and Planetary Change 26, 423–443.

Renssen, H., Lautenschlager, M., Schuurmans, C.J.E., 1996. The atmospheric winter circulation during the Younger Dryas stadial in the Atlantic/European sector. Climate Dynamics 12, 813–824.

Renssen, H., Isarin, R.F.B., Vandenberghe, J., Lautenschlager, M., Schlese, U., 2000. Permafrost as a critical factor in palaeoclimate modelling: the Younger Dryas case in Europe. Earth and Planetary Science Letters 176, 1–5.

Rind, D., Peteet, D., 1985. Terrestrial conditions at the Last Glacial Maximum and CLIMAP sea surface temperature estimates: are they consistent? Quaternary Research 24, 1–22.

Rind, D., Peteet, D., Broecker, W., McIntyre, A., Ruddiman, W., 1986. The impact of cold North Atlantic sea surface temperatures on climate: implications for the Younger Dryas cooling (11–10 k). Climate Dynamics 1, 3–33.

Roeckner, E., Arpe, K., Bengtsson, L., Brinkop, S., Dümenil, L., Esch, M., Kirk, E., Lunkeit, F., Ponater, M., Rockel, B., Sausen, R., Schlese, U., Schubert, S., Windelband, M., 1992. Simulation of the present-day climate with the ECHAM model: impact of model physics and resolution. Max Planck Institut für Meteorologie report no. 93, Hamburg, 172 pp.

Roeckner, E., Arpe, K., Bengtsson, L., Christoph, M., Claussen, M., Dümenil, L., Esch, M., Giorgetta, M., Schlese, U., Schulzweida, U., 1996. The atmospheric general circulation model ECHAM-4: model description and simulation of present-day climate. Max-Planck-Institute für Meteorologie report no. 218, Hamburg, 90 pp.

Rybnickova, E., 1974. Die Entwicklung der Vegetation und Flora im südlichen Teil der Böhmisch-Märischen Höhe während des Spätglazials und Holozäns. Vegetace CSSR A 7, 163 pp.

Sarnthein, M., Jansen, E., Weinelt, M., Arnold, M., Duplessy, J.C., Erlenkeuser, H., Flatøy, A., Johannessen, G., Johannessen, T., Jung, S., Koç, N., Labeyrie, L., Maslin, M., Pflaumann, U., Schulz, H., 1995. Variations in Atlantic surface ocean paleoceanography, 50°–80°N: a time-slice record of the last 30,000 years. Paleoceanography 10, 1063–1094.

Saunders, G.E., 1973. Vistulian periglacial environments in the Lleyn Peninsula. Biuletyn Peryglacjalny 22, 257–269.

Schiller, A., Mikolajewicz, U., Voss, R., 1997. The stability of the North Atlantic thermohaline circulation in a coupled ocean–atmosphere general circulation model. Climate Dynamics 13, 325–347.

Schulz, H., 1995. Meeresoberflächentemperaturen vor 10.000 Jahren—Auswirkungen des frühholozänen Insolationsmaximum. Berichte—Reports, Geologisches-Paläontologische Institut Universität Kiel 73, 156 pp.

Severinghaus, J.P., Brook, E.J., 1999. Abrupt climate change at the end of the last glacial period inferred from trapped air in polar ice. Science 286, 930–934.

Stalling, H., 1987. Untersuchungen zur spät-und postglazialen Vegetationsgeschichte im Bayerischen Wald, Dissertation Univ. Göttingen, 153 pp.

Tarasov, P.E., Harrison, S.P., Saarse, L., Pushenko, M.Ya., Andreev, A.A., Aleshinskaya, Z.V., Davydova, N.N., Dorofeyuk, N.I., Efremov, Yu.V., Khomutova, V.I., Sevastyanov, D.V., Tamosaitis, J., Uspenskaya, O.N., Yakushko, O.F. and Tarasova, I.V, Ya, M., Elina, G.A., Elovicheva Ya.K., Filimonova, L.V., Gunova, V.S., Kvavadze, E.V., Nuestrueva, I.Yu., Pisareva, V.V., Shelekhova, T.S., Subetto, D.A., and Zernitskaya, V.P., 1996. Lake status records from the former Soviet Union and Mongolia. Database documentation Version 2. IGBP/World Data Center-A for Paleoclimatology. Data Contribution Series # 96-032. NOAA/NGDC Paleoclimatology Program, Boulder Co, USA.

Taylor, K.C., Lamorey, G.W., Doyle, G.A., Alley, R.B., Grootes, P.M., Mayewski, P.A., White, J.W.C., Barlow, L.K., 1993a. The "flickering switch" of late Pleistocene climate change. Nature 361, 432–436.

Taylor, K.C., Hammer, C.U., Alley, R.B., Clausen, H.B., Dahl-Jensen, D., Gow, A.J., Gundestrup, N.S., Kipfstuhl, J., Moore, J.C., Waddington, E.D., 1993b. Electrical conductivity measurements from the GISP2 and GRIP Greenland ice cores. Nature 366, 549–552.

Valdes, P.J., Hall, N.M.J., 1994. Mid-latitude depressions during the last ice-age. In: Duplessy, J.-C., Spyridakis, M.-T. (Eds.), Long-term Climatic Variations. NATO ASI Series, vol. I (22), Springer-Verlag, Berlin, pp. 511–531.

Valero-Garcés, B., Zeroual, E., Kelts, K., 1998. Arid phases in the western Mediterranean region during the last glacial cycle reconstructed from lacustrine records. In: Benito, G., Baker, V.R., Gregory, K.J. (Eds.), 1998. Palaeohydrology and Environmental Change, vol. 353, Wiley, Chichester, pp. 67–80.

Van der Knaap, W.P., Van Leeuwen, J.F.N., 1997. Late Glacial and early Holocene vegetation succession, altitudinal vegetation zonation and climatic change in the Serra da Estrella, Portugal. Review of Palaeobotany and Palynology 97, 239–285.

Vandenberghe, J., Pissart, A., 1993. Permafrost changes in Europe during the last Glacial. Permafrost and Periglacial Processes 4, 121–135.

Vandenberghe, J., Kasse, C., Bohncke, S., Kozarski, S., 1994. Climate-related activity at the Weichselian–Holocene transition: a comparative study of the Warta and Maas rivers. Terra Nova 6, 476–485.

Van Vliet-Lanoe, B., Fagnart, J.P., Langohr, R., Munaut, A., 1992. Importance de la succession des phases écologiques anciennes et actuelles dans la différentation des sols lessivés de la couverture loessique d'Europe occidentale: argumentation stratigraphique et archéologique. Science de Sol 30, 75–93.

Von Grafenstein, U., Erlenkeuser, H., Brauer, A., Jouzel, J., Johnsen, S., 1999. A Mid-European decadal isotope-climate record from 15,000 to 5000 years B.P. Science 284, 1654–1657.

Walker, M.J.C., 1982. The Late-glacial and early flandrian deposits at Traeth Mawr, Brecon Beacons, South Wales. New Phytologist 90, 177–194.

Walker, M.J.C., 1995. Climatic changes in Europe during the Last Glacial/Interglacial transition. Quaternary International 28, 63–76.

Walker, M.J.C., Harkness, D.D., 1990. Radiocarbon dating the Devensian Lateglacial in Britain: new evidence from Llanilid, South Wales. Journal of Quaternary Science 5, 134–144.

Wastegård, S., Björck, S., Possnert, G., Wohlfarth, B., 1998. Evidence for the occurrence of Vedde Ash in Sweden: radiocarbon and calendar age estimates. Journal of Quaternary Science 13, 271–274.

Watts, W.A., 1977. The Late Devensian vegetation of Ireland. Philosophical Transactions of the Royal Society of London B 280, 273–293.

Watts, W.A., Allen, J.R.M., Huntley, B., Fritz, S.C., 1996. Vegetation history and climate of the last 15,000 years at Laghi di Montecchio, southern Italy. Quaternary Science Reviews 15, 113–132.

Webb, R.S., Anderson, K.H., Webb III, T., 1993. Pollen response-surface estimates of Late-Quaternary changes in the Moisture Balance of the Northeastern United States. Quaternary Research 40, 213–227.

Wegmüller, S., Lotter, A.F., 1990. Palynostratigraphische Untersuchungen zur spät-und postglazialen Vegetationsgeschichte der nordwestlichen Kalkalpen. Botanicae Helvetica 100, 37–73.

Weinelt, M., Sarnthein, M., Pflaumann, U., Schulz, H., Jung, S., Erlenkeuser, H., 1996. Ice-free Nordic seas during the Last Glacial Maximum? Potential sites for deepwater formation. Palaeoclimates 1, 283–309.

Wohlfarth, B., 1996. The chronology of the last termination: a review of radiocarbon-dated, high resolution terrestrial stratigraphies. Quaternary Science Reviews 15, 267–284.

Wright Jr., H.E., Kutzbach, J.E., Webb III, T., Ruddiman, W.F., Street-Perrott, F.A., Bartlein, P.A., 1993. Global Climates since the Last Glacial Maximum. University of Minnesota Press, Minneapolis, 579 pp.

Yu, G., Harrison, S., 1995. Lake Status Records from Europe. Database Documentation. IGBP PAGES/World Data Center-A for Paleoclimatology Data Contribution Series # 95–009, NOAA/NGDC. Paleoclimatology Program, Boulder CO, USA.

Zagwijn, W.H., 1994. Reconstruction of climate change during the Holocene in western and central Europe based on pollen records of indicator species. Vegetation History and Archaeobotany 3, 65–88.

Zazo, C., Goy, J.L., Lario, J., Silva, P.G., 1996. Littoral zone and rapid climatic changes during the last 20,000 years.The Iberia study case. Zeitschrift für Geomorphologie 102, 119–134.